Science of the Total Environment 724 (2020) 138287

Contents lists available at ScienceDirect

Science of the Total Environment

journal homepage: www.elsevier.com/locate/scitotenv

Putting the poorly documented 1998 GLOF disaster in Shakhimardan River valley (Alay Range, Kyrgyzstan/Uzbekistan) into perspective

Dmitry A. Petrakov [a,*], Sergey S. Chernomorets [a], Karina S. Viskhadzhieva [a], Mikhail D. Dokukin [b], Elena A. Savernyuk [a], Maxim A. Petrov [c], Sergey A. Erokhin [d], Olga V. Tutubalina [a], Gleb E. Glazyrin [e], Alyona M. Shpuntova [a], Markus Stoffel [f,g,h]

[a] Lomonosov Moscow State University, Leninskiye Gory, 119991, Moscow, Russia
[b] High-Mountain Geophysical Institute, Nalchik, Russia
[c] Institute of Geology and Geophysics, National Academy of Sciences of Uzbelistan, Tashkent, Uzbekistan
[d] Kyrgyz State Agency of Geology and Institute of Water Problems and Hydropower, National Academy of Sciences of Kyrgyz Republic, Bishkek, Kyrgyzstan
[e] National University of Uzbekistan, Tashkent, Uzbekistan
[f] Climatic Change Impacts and Risks in the Anthropocene (C-CIA), Institute for Environmental Sciences, University of Geneva, Switzerland
[g] dendrolab.ch, Department of Earth Sciences, University of Geneva, Switzerland
[h] Department F.-A. Forel for Environmental and Aquatic Sciences, University of Geneva, Switzerland

HIGHLIGHTS

- We provide the first detailed assessment of the deadliest historical GLOF in Central Asia.
- The "Shakhimardan" disaster of 1998 was presumably triggered by an outburst of small lakes.
- Significant erosion and entrainment of loose material is observed even in sections with slope angles <8°.
- An updated mountain lake inventory of the Shakhimardan catchment shows that the disaster could repeat.

GRAPHICAL ABSTRACT

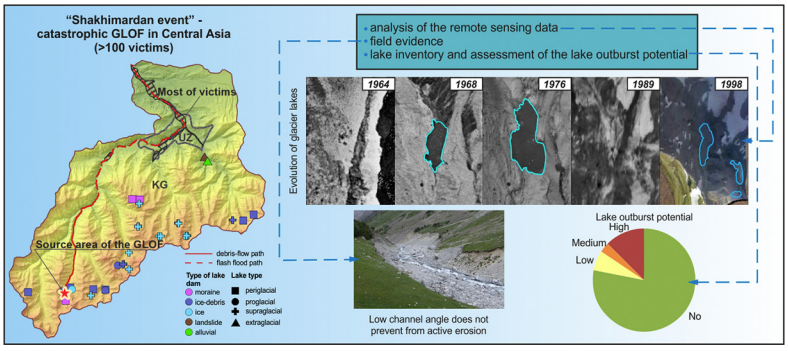

ARTICLE INFO

Article history:
Received 17 December 2019
Received in revised form 26 February 2020
Accepted 26 March 2020
Available online 31 March 2020

Editor: Damia Barcelo

Keywords:
Glacier lake outburst flood (GLOF)
Shakhimardan disaster
Alay range

ABSTRACT

On July 8, 1998, the deadliest glacier lake outburst flood (GLOF) in Central Asia for at least the last 100 years occurred in the Shakhimardan catchment, Kyrgyzstan. Most of the >100 victims were, however, killed in the Uzbek enclave of Shakhimardan, i.e. in the downstream part of this transboundary catchment. No warnings were issued between the two countries. In addition, due to political tensions, access to the site was impossible and a detailed assessment of the disaster could not be realized until now. Using remote sensing, we show that the lake at the origin of the "Shakhimardan event" appeared in the 1960s and drained periodically, without, however, causing damage to downstream areas before it eventually disappeared in the late 1980s. Based on post-event videos, we conclude that the GLOF-producing depression was again filled with a lake, estimated at $20 \pm 1.2 \times 10^3$ m^2 in area, before the disaster. The lake burst was likely driven by the rapidly rising air temperatures and the melting of snow/ice in late June and early July. The GLOF first travelled as a debris flow for 17 km, then continued as a debris flood in the increasingly flatter channel for another 20 km. Interestingly, the mean weighted channel angle in the areas of erosion was extremely low at 6.7°. The flood continued further downstream for ~100 km from its

* Corresponding author.
E-mail address: dpetrakov@gmail.com (D.A. Petrakov).

https://doi.org/10.1016/j.scitotenv.2020.138287

source. Today, 32 lakes (total area ~300 × 10^3 m^2 in 2018) exist in the catchment, with several of the larger lakes (>5 × 10^3 m^2) showing signs of instability. We therefore call for a systematic monitoring of environments like the Shakhimardan catchment, as well as for the installation of early warning systems at critical sites, with exchange of data between the Kyrgyz and Uzbek disaster risk management units, so as to mitigate existing and evolving GLOF risks.

1. Introduction

The ongoing climate warming (Hock et al., in press; Hu et al., 2014) and the related, yet spatially heterogeneous glacier shrinkage that has recently been observed in Central Asia (Brun et al., 2017; Farinotti et al., 2015; Hoelzle et al., 2019; Sorg et al., 2012) favored the formation and rapid growth of glacier lakes (Engel et al., 2012; Janský et al., 2009; Mergili and Schneider, 2011; Wang et al., 2013; Zheng et al., 2019). Even if the Central Asian lakes typically have much smaller volumes compared to their counterparts in the Hindukush-Karakoram-Himalayan (HKH) region (Narama et al., 2010; Worni et al., 2013; Schwanghart et al., 2016), they have more frequently favored the occurrence of GLOFs and hydrogeomorphic disasters downstream of their source. This difference in the occurrence of GLOFs and their negative consequences is explained by the fact that a vast majority of GLOFs in the Central Asian region transform into destructive debris floods or debris flows as they move down steep terrain covered with loose sediment. Over the last decades alone, Central Asian GLOFs and the resulting debris flows have killed hundreds of people and destroyed numerous houses, farmland surfaces and tourist infrastructure in Central Asia (Mergili and Schneider, 2011; Narama et al., 2010, 2018; UNEP, 2007; Yafyazova, 2007).

In addition, and unlike their counterparts in the HKH, where historical disasters remain comparably scarce (Worni et al., 2013; Schwanghart et al., 2016; Allen et al., 2019), Central Asia has seen a substantial number of 20th century, well-documented GLOF events, especially originating from lakes located in the Northern Tien Shan. Here, most of the 50 documented GLOFs occurred between the 1960 and 1990s (Stepanov and Yafyazova, 1995, 2001; Vinogradov, 1969; Kapitsa et al., 2017), often coinciding with phases of glacier stagnation or slight glacier advances (Zaginaev et al., 2016, 2019). Repeatedly, the GLOFs transformed into debris flows with discharges of up to an estimated 12,000 m^3/s and volumes of entrained sediment of up to few million m^3 (Medeu, 2011). A debris flow disaster occurred in the Northern Tian Shan on 15 July 1973; the event was initiated by an outburst of two lakes with a total volume of just 225,000 m^3, but resulted in a discharge of 10,000 m^3/s and debris-flow deposits of about 4 × 10^6 m^3 (Yafyazova, 2007). The most recent GLOFs on record occurred in 2002 in the Western Pamirs (Mergili and Schneider, 2011), in 2008 in Terskey Alatoo (Narama et al., 2010) and in 2012 in Kyrgyz Alatoo ranges (Erokhin et al., 2018). Table 1 provides an overview of catastrophic GLOFs in Central Asia.

The deadliest GLOF and debris flow disaster in Central Asia occurred on 7 July 1998 on the territories of Kyrgyzstan (Batken Region) and Uzbekistan (Ferghana Region). The transboundary nature of this disaster prevented timely alerts and resulted in increased tensions between the two nations. >100 people were killed by the disaster that has often been referred to as the "Shakhimardan event" after the settlement that was the most affected. An estimated 500–600 persons were reported missing (ICRC, 1998), some 14,000 people had to be evacuated, 500 lost their houses, mostly in Uzbekistan, and the homes of at least 5000 Kyrgyz citizen were severely damaged (Reuters, 1998). As a result of the political tensions, post-event activities were restricted to a helicopter reconnaissance (Glazyrin, 1998). A scientific assessment of the events and/or an inspection of the headwaters of the Aksu catchment was not possible in the past due to tensions between the two countries that were exacerbated further by the disaster.

According to this helicopter reconnaissance (Glazyrin, 1998), a catastrophic debris flow would have formed following the outburst of three glacier lakes located in stagnant ice of the Archa-Bashi Glacier. The report also estimated lake morphometry and total lake volume (4000 m^3) during the overflight. It also stated that in early July 1998, only days before the disaster, the high mountains of the Alai Range were under the influence of a massive heatwave. At Abramov Glacier weather station, located at 3837 m a.s.l. at a distance of 11 km from Archa-Bashi Glacier, daily mean temperatures were rising from 7 °C to

Table 1
Overview of catastrophic GLOFs events in Central Asia. Note that data on victims might be not robust because they were kept secret during the Soviet period. MDFD = maximum debris flow discharge; DFV = debris flow volume.

Date	Location	River (basin), mountain range	Victims	Other information	Sources
July 7, 1963	Lake near the Jarsay Glacier and Issyk Lake, Esik town (Kazakhstan)	Issyk River (Ili River basin), Ile Alatau (North Tien Shan)	52	Esik town; 2 streets destroyed. MDFD: 7–12,000 m^3/s DFV: 5.8 million m^3	Yafyazova, 2007
July 15, 1973	Lake No. 2 near the Central Tuyuksu Glacier, Almaty (Kazakhstan)	Kishi Almaty River (Ili River basin), Ile Alatau (North Tien Shan)	70	MDFD: 10,000 m^3/s DFV: 3.8 million m^3	Yafyazova, 2007
August 3–4, 1977	Lake No. 13 near the Sovetov Glacier, Almaty (Kazakhstan)	Kumbelsu River (Ili River basin), Ile Alatau (Northern Tien Shan)	unknown	MDFD: 10,000 m^3/s DFV: 2.4–3.2 million m^3	Yafyazova, 2007
July 8, 1998	Lake near the Archa-Bashi Glacier, Shakhimardan exclave (Uzbekistan) and Kadamjay District (Kyrgyzstan)	Shakhimardan River (Syr Darya River basin), Alai Range	100	Property damage 700 million US$	*Mitigating the Adverse Financial Effects of Natural Hazards on the Economies of Central Asia: A Study of Catastrophe Risk Financing Options*, 2009
August 7, 2002	Lake near the Dasht Glacier, Roshtkala District (Tajikistan)	Shakhdara River (Amu Darya River basin), Pamir	23 (24) people	75 houses destroyed; 501 people without shelter. DFV: 1.0–1.5 million m^3	Mergili et al., 2011; IFRC, 2003; UNEP, 2007
July 24, 2008	Western Zyndan Lake near the Western Zyndan Glacier, Tong District (Kyrgyzstan)	Zyndan River (Tong River Basin), Teskey Ala-Too Range (Central Tien Shan)	3	Discharged water volume: 0.437 million m^3	Narama et al., 2010

12 °C. During the post-event reconnaissance on July 8, 1998, air temperature was still 15 °C at 5 PM local time at an elevation of *c.* 4000 m a.s.l. Glazyrin (1998) therefore concluded that this episode of abrupt warming would have led to a rapid melting of ice and snow and to a rapid filling of the lakes with abundant meltwater.

The initial assessment also concluded that the disaster started from the uppermost and largest of the three lakes (Fig. 1) and as a result of the failure of an ice-debris dam, which then would have allowed the burst of the lake into the lower lakes, thereby leading to a chain reaction. Discharge of the initial outburst was estimated at 2–3 m^3/s. On its way downstream, the flood wave entrained considerable amounts of sediment and larger debris through massive bank and bed erosion such that the flood was consequently transformed into a debris flow. Enough water was added to the flow by numerous tributaries with significant meltwater discharge as well as by eroded, water-saturated soils. Once reaching the settlement of Shakhimardan, the flow was estimated to have had a discharge of about 150–200 m^3/s (Fig. 1).

Due to the political tensions and despite the fact that the "Shakhimardan event" was the deadliest GLOF in Central Asia of the last 100 years (no reliable data exists for earlier periods), the disaster has not been studied in detail so far, and all conclusions, although very vague, have been drawn on the basis of the post-event report prepared after helicopter reconnaissance. As such, the role of the sudden warming and/or the lakes in the disaster remained largely unclear. How could so much water be mobilized during the event, and where did it come from? What triggered the "Shakhimardan event" and how did the lakes evolve prior to the outbreak? How did erosion, transport and accumulation processes interact along the channel, and how could the small lakes transform into such a large event? We also note that problems with transboundary GLOFs/glacier related hazards may not just arise between Kyrgyzstan and Uzbekistan but also between Kyrgyzstan and Tajikistan, Afghanistan and/ Tajikistan, China and India, China and Nepal as well as in many other regions (e.g. Allen et al., 2019). The observed global shrinkage of glaciers has caused new lakes to form and existing lakes to grow in most glaciated regions, including High-Mountain Asia (Hock et al., 2019), where new "hot spots" of glacier risks are forming. Downstream countries are especially vulnerable to GLOFs due to the lack of warning systems, therefore calling for international collaboration aimed at mitigating transboundary impacts of glacier hazards (Rasul et al., 2019).

Based on the above considerations, the specific goals of this study therefore are to (i) explore the evolution of the glacier lakes and their surroundings prior to the "Shakhimardan event"; (ii) identify geomorphic features left by the catastrophic flow of 1998 using remote sensing data and field evidence; (iii) clarify the role of the weather anomalies, glacier evolution, seismicity and/or rock avalanches in triggering the lakes to burst and the chain of processes to evolve; and to (iv) understand current and possible future GLOF hazards in the Shakhimardan River catchment.

2. Physical geography of the study area

The Shakhimardan River and its catchment form a transboundary fluvial system which crosses the border between Kyrgyzstan and Uzbekistan multiple times. As shown in Fig. 2, the headwaters of the river (with a length of 34 km) are located in the Batken region of Kyrgyzstan, then it flows into the Shakhimardan enclave in the Fergana region, Uzbekistan, to enter again into the Batken region of Kyrgyzstan after 14 km. After another 21 km in Kyrgyzstan, the Shakhimardan river flows back into Uzbek territory where it ends in the Syr Daria river at a distance of 121 km from its source. Mean water discharge of the Shakhimardan river is ~10m^3/s, and a large part of its waters is diverted to the Great Ferghana Channel where it is used for agricultural purposes. The Shakhimardan river is a typical mountain river draining northern slopes of the Alai Range, a W-E stretching mountain chain consisting of flyschoidal strata of Paleozoic continental-marine formations, interbedded sandstones and shales, with intrusions of granites and gneisses (Tulyaganov et al., 1980). Quaternary deposits are abundant and formed primarily by till, fluvioglacial, alluvial, proluvial and colluvial sediments.

The highest summit of the Shakhimardan catchment is Tashkent peak with an elevation of 5259 m a.s.l. The valley bottom reaches altitudes of 3600 m a.s.l. in the headwaters, and decreases to 1400 m a.s.l. at Shakhimardan settlement. The headwaters of the catchment are characterized by valley, cirque and niche glaciers with a total area of about 35 km^2 remaining today, and with glacier termini at 3500–3700 m a.s.l. Debris-covered ice predominates on the glacier snouts. Glacier mass exchange is quite high for continental regions with an estimated 1–1.5 $m \cdot a^{-1}$ of accumulation and ablation at the level of the equilibrium line altitude (ELA) at 4200 m a.s.l, (*World Atlas of Snow and Ice Resources,* 1997). Rock glaciers are widespread at altitudes between 3300 and 4000 m a.s.l. Most rock glaciers are still active and some are partially damming the main tributary rivers. Past glaciations have left characteristic U-shaped valleys in the study region, which have since been altered by active tectonics and massive sedimentation by debris flows and talus processes, covering bedrock in thick, loose and easily erodible Quaternary deposits.

Climate of the region is continental, with annual precipitation at high elevations estimated at 500–1000 mm (Voloshina, 2002), and <500 mm in Ferghana depression. The majority of precipitation falls during late spring and early summer. Mean annual air temperature is −3.7 °C at 3837 m a.s.l. (Barundun et al., 2015) and 1.9 °C at 3000 m a.s.l. (Radchenko et al., 2017). Steppe vegetation predominates in the valley bottoms below 2700 m. At higher elevations, meadows and steppes with intermittent *Juniperus* forests occur, to be themselves replaced by alpine meadows and the glacial-nival belt above 3500 m.

All torrents and rivers in the valley are fed by glaciers and rock glaciers, in addition to melting snow (*World Atlas of Snow and Ice Resources,* 1997). The "Shakhimardan disaster" originated on the

Fig. 1. Detailed view of the lakes located downstream of Archa-Bashi Glacier immediately after the outburst (left). Destruction of Shakhimardan settlement and accumulated debris (right). Archived footage from the Associated Press (Associated Press, 1998).

Fig. 2. Location map of the study area in the transboundary Shakhimardan catchment: 1 – starting zone of the debris flow (1998); 2 –Shakhimardan River and path of the 1998 debris flow, 3 – outline of the area investigated in the field study.

Allaudin river. After its confluence with the Karakazyk and Ikedavan rivers farther down, the river changes its name to Aksu River. At the confluence of the Aksu (White) with the Koksu (Blue) rivers, upstream of Shakhimardan settlement, the river is named Shakhimardan (Kosarev, 1954). According to the authors' analysis of topographic maps and DEMs, the drainage in the catchment is generally from S to N, and slope angles of the Shakhimardan river system decrease as its waters are flowing N: in the headwaters, steeper segments (8–10°) interchange with flat areas (2–3°); between the source of the tributaries and the settlement, slope angles are 2.5–4° on average; and in the downstream area, near Shakhimardan settlement, angles are in the range of 1.5–2.5°. The width of the river valley varies between 40 and 200 m.

3. Materials and methods

3.1. Time-series analysis of aerial photographs and satellite imagery

Multiple sets of aerial photographs and satellite imagery were used to detect change in and around the initiation and transit zones of the GLOF and debris flow before and after 1998. The list of images used to this end is presented in Table 2. The main goal of this analysis was to estimate the approximate extent of the lakes before the outburst and to appraise the water volume released during the outburst. The evolution of the lakes has therefore been traced back to 1964. In addition, historical images have been used to identify debris-flow deposits that could have formed as a result of lake outburst. The most recent images, taken after the "Shakhimardan event", have been screened to identify lakes existing today, debris flow channels, glaciers and rock glaciers, with the aim to assess GLOF and/or debris-flow hazards in the Shakhimardan catchment under present-day conditions.

All images and maps were transformed into 1984 WGS UTM zone N40 projection before they were co-registered using the Sentinel 2 MSI image taken on 28 August 2018 as a master image. This intermediate step was necessary because high resolution images, like Ikonos, did not provide the nadir view. A total of 150 to 300 control points (depending on image resolution and shooting angle) were selected for the co-registration of images. Two scanned Soviet topographic maps from the 1980s (at the scale of 1:50,000) and a digital elevation model (DEM) from the Shuttle Radar Topography Mission (SRTM3) were used for orthorectification of the satellite and aerial data in ArcGIS software. Images from the initiation zone taken during the helicopter reconnaissance (i.e. helicopter-based video) were integrated into this GIS as well. In the case of helicopter images with a rather low resolution, we only selected 80 control points. Whereas the first points were co-registered manually, the ArcGIS-Spline tool (Zhang et al., 2016) was then used to transform output control points to target control points. The Swipe Layer tool helped in checking planar coordinate difference between control points. We used multiple corrections to receive minimal residual errors. All images were free of clouds and taken during summer or early autumn when periglacial landforms are the most visible because of limited snow extent. All interpretations of images, the delineation of landforms and calculations were realized in ArcGIS 10.2. Regarding delineation accuracy for lake banks and boundaries of debris-flow tracks, we assume that the maximum error of area determination is in the order of half a pixel (O'Gorman, 1996; Pieczonka and Bolch, 2015; Petrakov et al., 2016). For each object, this error has been assessed by buffering the object perimeter by a half-pixel mask so as to determine the area uncertainty.

3.2. Geomorphic field mapping in 2014

A field mission and a geomorphic mapping campaign were realized on 8–18 July 2014 to document remaining evidence of the "Shakhimardan event" and to retrace the GLOF path in the Aksu river valley. In addition to in-situ geomorphic descriptions, cross-section profiles were measured with a Bushnell G-Force 1300 ARC laser rangefinder and traces of the 1998 disaster documented with photography. We also interviewed eye witnesses on the dynamics of the GLOF and the ensuing debris-flow event.

On the basis of the geomorphic descriptions we then delineated different lithodynamic zones (Chernomorets, 2005) along the debris-flow path. Lithodynamic zones are defined here as sectors of the river bed and adjacent slopes characterized by differing mass budgets (inputs) during debris-flow events; they comprise erosional, transit-erosional, transit, transit-accumulation, and accumulation zones from the rock glacier terminus down to the Gadzhir river mouth (Fig. 3), where the debris flow changed into a debris flood. In addition, morphometric measurements (i.e. length, width) have been made within each of the lithodynamic zones. Limits between zones were geolocated with a

Table 2
Aerial and satellite images, topographic maps and DEMs used in this study.

Data	Date	Resolution, m or scale	Sources, authors
Aerial images	06.08.1976; 30.09.1989	1:15000, 1:25000	
KH-4A	19.10.1964;	2.7–7.6	USGS
KH-4B	18.08.1968; 15.09.1971	1.8	http://earthexplorer.usgs.gov/
KH-9	08.07.1980; 20.08.1980	6–12	
Landsat 5TM	14.06.1991; 17.08.1992; 20.10.1992; 03.07.1993; 19.07.1993; 20.08.1993; 21.09.1993; 04.06.1994; 20.06.1994; 22.07.1994; 24.07.1994; 23.08.1994; 10.10.1994; 06.05.1995; 02.10.1997; 15.10.1997; 18.10.1997; 30.05.1998; 15.07.1998; 02.08.1998; 03.09.1998; 16.09.2000	30	
Landsat 7 ETM+	22.09.2000	30/15[a]	
Landsat 8 OLI	13.07.2014	30/15[a]	
SRTM 90	02.2000	90	Consortium for Spatial Information (CGIAR-CSI), SRTM 90 m Digital Elevation Database v4.1, http://www.cgiar-csi.org/data/srtm-90m-digital-elevation-database-v4-1
WorldView-2	10.07.2013	1,84/0,5[a]	ESRI, World Map http://goto.arcgisonline.com/maps/World_Imagery
Ikonos	19.07.2007, 05.10.2013	3,28/0,82[a]	DigitalGlobe. https://www.google.ru/maps/@39.8724701,71.8021581,45292m/data=!3m1!1e3?hl=ru
Sentinel 2B	28.08.2018	10	Copernicus Open Access Hub https://scihub.copernicus.eu/dhus/#/home
ALOS PALSAR DEM	22.07.2007	12.5	Alaska Satellite Facility https://vertex.daac.asf.alaska.edu/
Soviet military topographic maps	j42–012–2; j42–012-3	1:50000	
Aerial video	09.07.1998 (the day after debris flow		Associated Press…, 1998
Aerial photos	August 1998		S. Erochin

[a] Resolution of multispectral/panchromatic imagery.

Garmin GPSmap 60Csx receiver using the 1984 WGS UTM zone N40 projection and adjusted during postprocessing with an Ikonos satellite image of 2013. Uncertainty of delineations was about 10 m in most cases. At sites where limits between zones were unclear, uncertainty increased to 30–40 m locally.

Thereafter, topographic maps at a scale of 1:50000 (compiled in 1982) were used to estimate slope angles in the identified zones. Assessment of the slope angles left after the passage of the debris flow were determined with a smooth centerline drawn along the valley bottom. In the remote areas of Central Asia, estimates derived from topographic maps remain more accurate than open-access DEMs, in addition, they reflect the terrain prior to the passage of the 1998 debris flow, whereas all available DEMs provide information about the situation after the event only. During the "Shakhimardan event", the debris flow covered much of the valley bottom during its passage in a straight flow, whereas recently, the river has started to form meanders, especially in the zones where debris-flow material was accumulated in 1998. By contrast, in the erosional and transit zones, meandering is virtually absent. In addition, and where possible, we also assessed the thickness of the 1998 debris-flow deposits.

3.3. Estimation of lake volume, lake outburst, debris-flow discharge and flow velocity

The volume of the glacier lake could not be measured prior to the outburst, and the helicopter-based assessments suffer from inaccuracies and limited image quality. In addition, the resolution of the DEMs obtained for the 1990s was not of sufficient quality either to assess the volume of depressions (i.e. sinks) on the moraine complex. We therefore assessed lake volume with the empirical equations proposed by Huggel et al. (2002) as well as with graphs designed for volume estimates of short-lived lakes (Narama et al., 2018, Fig. 9). In the first case, the authors suggested that

$$V = 0.104A^{1.42}$$

where V is lake volume (in m^3) and A is lake area (in m^2). In the case of englacial or subglacial drainage from lakes, Walder and Costa (1996) calculated maximum discharge Q_{max} as follows:

$$Q_{max} = 46\left(V/10^6\right)^{0.66}$$

where V is lake volume (in m^3). In the case of the "Shakhimardan event", the outburst was caused by a failure of the moraine dam. A narrow slit observed after the GLOF indicates that ice content in moraine was significant. Therefore, a more simple equation can be used for ice- and moraine dam failures. In the case of ice dams, the following equation has been suggested:

$$Q_{max} = V/t$$

where V is lake volume (in m^3), and t is the drainage duration in seconds. For applications in practice, it is recommended to use $t = 1000$s. In the case of moraine dams,

$$Q_{max} = 2\,V/t$$

Considering the poor quality of the DEMs that could be used to assess channel angle, the least sophisticated approaches should be applied to evaluate debris-flow parameters. In this context, empirical equations as the ones developed during Soviet times can be used as they have proven quite accurate in Central Asia and whenever rough assessments

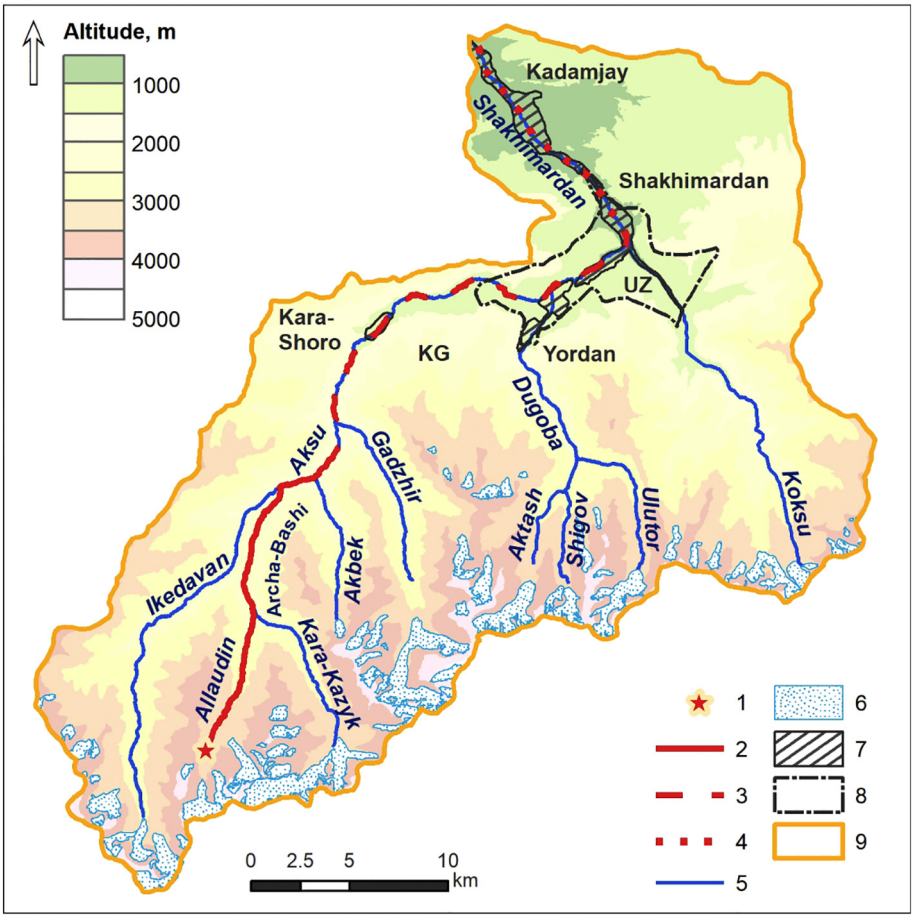

Fig. 3. Schematic map of the 1998 GLOF with debris flow and flash flood paths; 1 – source area of the GLOF that initiated the "Shakhimardan event" on July 8, 1998, 2 –debris-flow path, 3 – debris flood path, 4 – flash flood path, 5 – river channels, 6 – glaciers, 7 – settlements, 8 – boundaries of the Uzbek exclave of Shakhimardan, 9 – limits of the Shakhimardan catchment investigated in this study. Abbreviations: UZ – Uzbekistan, KG – Kyrgyzstan.

suffice. We therefore estimated debris flow velocity and discharge using equations of Kherkheulidze (1972).

$$V = 4.83 \cdot h^{0.5} \cdot I^{0.25},$$

$$Q = A \cdot V,$$

where V is debris-flow velocity (m/s), h is mean debris-flow depth (m), I is the channel angle (m/m), Q is debris flow discharge (m^3/s) and A is the area of the flow cross-section (m^2). To estimate velocity of the debris flood V we used equation proposed by Golubtsov (1969):

$$V = 4,5\, h^{0},67 I^{0},17$$

3.4. Mountain lake inventory and assessment of the lake outburst potential

The currently existing inventory of mountain lakes in Shakhimardan River catchment was created by Petrov et al. (2017) on the basis of very high-resolution satellite imagery (WorldView 2 with spatial resolution 0.5 m/pixel), obtained in 2007–2013. In that survey, four lakes with areas ranging from 1000 m^2 to 100,000 m^2 were identified in the catchment. Due to the rapid changes of periglacial areas in Central Asia (Sorg et al., 2012; Erokhin et al., 2018) and the availability of more recent, open access high-resolution (10 m/pixel) images from Sentinel 2 satellites, we provide a new lake inventory for Shakhimardan catchment and reassess the outburst potential of present-day lakes, with the aim to analyze whether a new disaster similar to the 1998 event could occur today.

To this end, we analyzed a Sentinel-2B MSI image acquired on 28 August 2018 (Table 2) with minimum snow cover, absence of clouds and high contrast. We used a Radiometrically Terrain Corrected (RTC) ALOS PALSAR DEM processed by the Alaska Satellite Facility with a spatial resolution of 12.5 m/pixel (ASF DAAC, 2015) to determine absolute lake heights, geometric parameters of dams, and to quantify possible depressions. As the most recent High Mountain Asia 8-m DEM (Shean, 2017) is of rather poor quality and has significant data voids for the Shakhimardan catchment, lakes had to be outlined manually in ArcGIS. An automatic interpretation based on band ratios (e.g., NDWI proposed by Huggel et al., 2002) to identify lakes was not used because the spectral reflectance of the lakes has been shown to vary and as sometimes the lake area was too small.

The lake inventory produced here includes the following parameters: lake ID, x/y coordinates for WGS84 UTM Zone 42, altitude (m a.s.l.), lake area (in m^2), name of the river catchment, lake type (with respect to its position relative to the glacier), dam type, freeboard (in m), connectivity between lakes, drainage type, potential for lake impacts (e.g., mass-movements falling into the lake), and outburst potential (for details see Table S1 in the Supplementary Material).

These parameters have been developed by Worni et al. (2013) and were used in Petrov et al. (2017); by using the same approach to assess the lake outburst potential we aim at rendering the assessments comparable over time. The qualitative and quantitative values obtained were then divided into three categories of outburst potential (low, medium, and high). The highest score (i.e. sum of all scores) in terms of outburst

probability has a value of 27, the lowest score has a value of 9. In cases where the score is <15 the lake has a low outburst probability (as calibrated with field data). By contrast, lakes with scores >21 are considered to have a high outburst probability.

Four types of lakes are distinguished here based on their position relative to the glacier: supraglacial lakes (located on the glacier itself or on dead ice), proglacial lakes (partly adjoining to a glacier or stagnant ice), periglacial lakes (located at distances <2 km from the glacier terminus) and extraglacial lakes (located at the distance exceeding 2 km from the present-day glacier terminus). Criteria for the identification of lake types are given in Petrov et al. (2017). Noteworthy, the distance threshold (2 km) used for the extraglacial or periglacial lakes was based on field evidence in the present case and therefore differs from the definition provided by Petrov et al. (2017).

Also, we identified five dam types in this study: four of these (i.e. ice, ice-debris, moraine, or landslide dam) correspond to those defined by Petrov et al. (2017). In our case, and based on field evidence, we added the category "alluvial dams" consisting of alluvial and debris-flow deposits (often corresponding to debris-flow cones and alluvial fans blocking the valley).

Although freeboard height is one of the most important parameters in outburst hazard assessments (Worni et al., 2013), its assessment remains a challenge with remotely-sensed data. Due to limitations related to the quality of the DEM that was available in this study, we assessed freeboard height qualitatively and approximately by qualifying it to either less or >1 m. In Table S1, a value of "1" simply means that freeboard height is <1 m.

Hydrological connectivity between lakes is defined here as the possibility of the outburst of one lake triggering the outburst of other lakes further downstream, a process that is often referred to as "cascading events" or "process chains" (Schauwecker et al., 2019). Drainage type is an additional factor influencing lake outburst susceptibility. Mountain lakes with a stable surface drainage are less susceptible to outburst than lakes with an underground drainage, this is due to the fact that underground channels can be blocked by thermokarst processes in moraines, rock glaciers or stagnant ice, such that the blockage can lead to lake overflow and subsequent lake outburst through erosion and breach formation (Erokhin et al., 2018).

Last but not least, potential lake impacts were defined following Worni et al. (2013) and included the following types and origins of earth surface processes that could impact a lake and lead to an impact wave: rockfall, avalanche, ice-fall, or debris flow. Whereas lake parameters were identified for all lakes inventoried, the assessment of outburst potential was restricted to lakes with areas >5000 m^2.

To assess the potential for formation of new mountain lakes in the Shakhimardan catchment, we identified depressions (so-called sinks) in the periglacial zone (Narama et al., 2017) with both automated and manual approaches. Automated assessments were realized with the "Flow Direction" and "Sink" tools available in the ArcGIS Toolbox (Spatial Analyst Tools/Hydrology; Bajjali, 2017). This approach yielded data on 2892 depressions. In the next step, the analysis was restricted to the altitudinal range for which lakes are found today, i.e. at altitudes between 3500 and 4300 m a.s.l., limiting the dataset to 1213 depressions. Further filtering and exclusion of depressions located outside the glacier and rock-glacier domains was then realized with satellite imagery, reducing the final GIS database to 171 depressions. In this paper, depressions are not included in the lake inventory, but the location of depressions should be consulted when it comes to the identification of new lakes in the future.

4. Results

Fig. 3 provides details on the "Shakhimardan event" from July 8, 1998 and the behavior of the flow along its path from the source area of lake outburst to the borders of the investigated part of Shakhimardan River catchment. The GLOF in the headwaters of the Allaudin river transformed quickly into a debris flow and travelled for approximately 17 km down the valley before the flow transformed into a debris flood between kilometers 17 and 37. Farther downstream, and over ~60 km, field evidence points to a transformation of the debris flood into a flash flood.

4.1. Evolution of the non-stationary glacier lake reconstructed from remotely sensed imagery

The "Shakhimardan event" started with a GLOF which then triggered a suite of chain reactions. We thus focus on the evolution of the lake prior to and after the catastrophic lake outburst using the aerial pictures and satellite imagery presented in Table 2 and shown in Fig. 4. The lake that was at the origin of the 1998 disaster has formed sometimes between 1964 and 1968. When first visible in 1968, lake area was $13.5 \pm 0.8 \cdot 10^3$ m^2. On the image of 1971, it is unclear whether the lake contained any water or whether it was emptied, but the lake depression is undoubtedly located at the same site. In 1976, the lake reached its maximum area with $32.2 \pm 0.7 \cdot 10^3$ m^2. In subsequent years (1976–1980), the lake area was reduced by ~50% and cannot be seen any more in the image taken in 1989. Likewise, the lake can no longer be found in the images available in the early 1990s. Before the outburst on July 8, 1998, the lake was obviously been dammed again by the same moraine ridge (Fig. 4) as in 1976 when the dam height has been evaluated as very low. Also, any evidence of lakes located before the GLOF-producing lake is absent on images taken prior to 1998.

The black feature going to the NW from the lake on the 1976 image (blue arrow at Fig. 4) can be interpreted as a surface runoff feature appearing at the surface after drainage of water through tunnels within the moraine dam. In the absence of any signs of dam destruction, it seems likely that water drained through the englacial channels without surface erosion, thereby also limiting peak discharge (Zaginaev et al., 2019). This assumption can be corroborated by the fact that geomorphic changes recorded between 1980 and 1989 are more significant than those seen on the images between 1976 and 1980 (Fig. 5) and when lake volume was reduced substantially. Based on these data, we have to assume that the moraine ridge has been intact prior to the 1998 event and that it was eroded during the disaster as suggested by the low-resolution video from the helicopter reconnaissance realized immediately after the GLOF (Table 2, Fig. 1). It is also possible to find evidence for such a chain of processes on the detailed aerial image from August 1998 displayed in Fig. 6.

Lake outlines for the situation in 1998 have been extracted from the helicopter video so as to obtain an idea on the situation prior and after the outburst. The total area of the lake involved in the disaster is estimated at $20 \pm 1.2 \times 10^3$ m^2. Before the outburst, the water level must have increased to overflow the dam. A breach was then formed by the overflowing water and subsequent regressive erosion. Whereas Fig. 4 points to a relatively stable dam during the 1960s through to the 1990s, a breach could still develop just prior to and/or on July 8, 1998. As the breach was quite narrow (according to video recordings, Fig. 6), we assume that the dam must have contained frozen debris, presumably with (some) ice lenses.

After the "Shakhimardan event", the lake had an area of $6.7 \pm 0.5 \times 10^3$ m^2 or roughly only a third of its size prior to the disaster. Two new lakes were found during the helicopter reconnaissance, yielding a total area of $10 \pm 0.9 \times 10^3$ m^2 for the three lake remnants (Fig. 4). Noteworthy, the small lower lakes appeared just after the outburst but could not be identified on any of the images or during the reconnaissance prior to the disaster. Also, it was not possible to identify any signs of lateral or vertical movements of the moraine dam and/or parts of the moraine complex underneath the dam of the GLOF-producing lake between the 1960s and 1990s. The moraine dam has neither been massively eroded nor were the channels inside the dam and in the moraine complex blocked completely during the outburst.

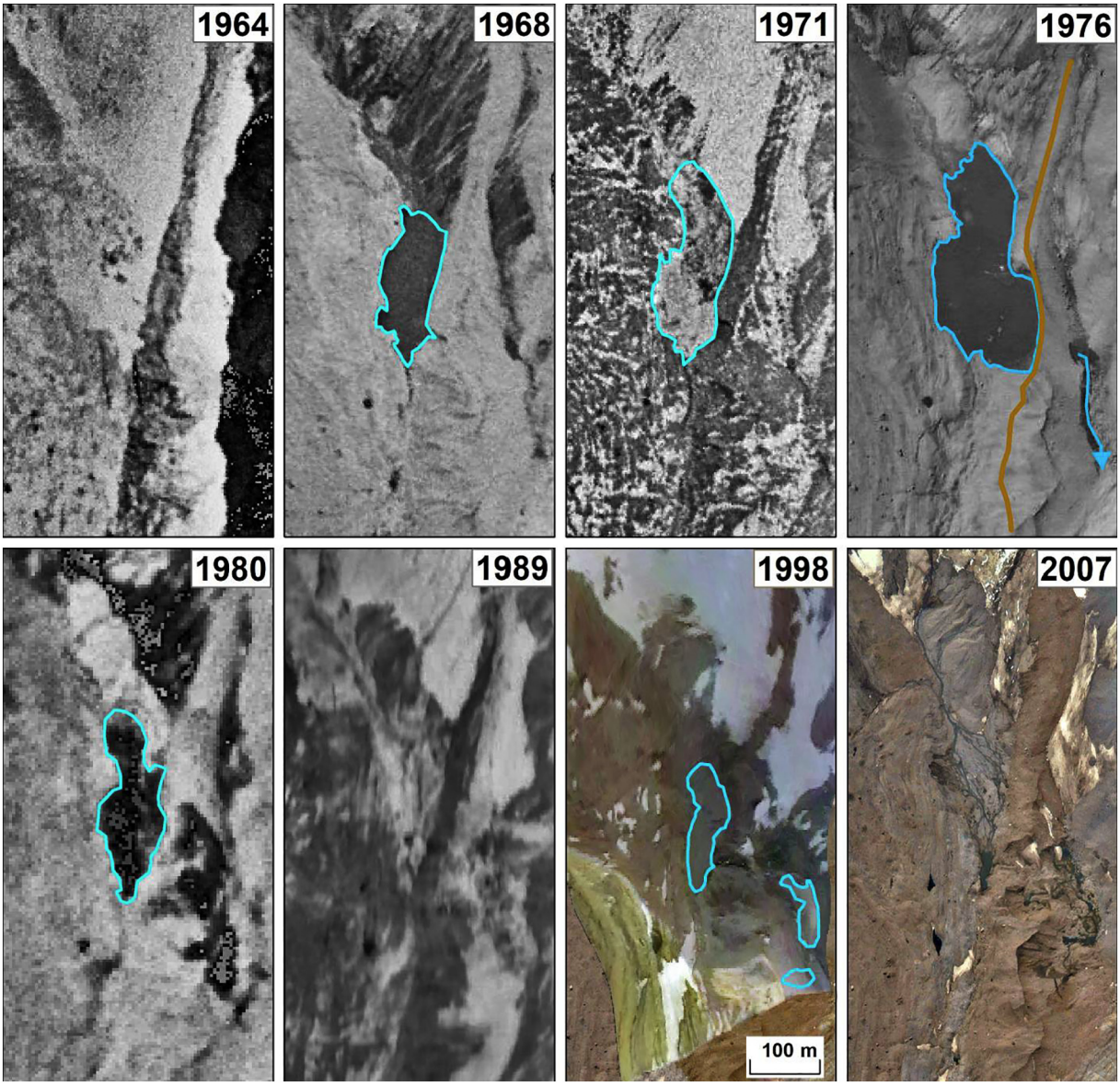

Fig. 4. Initiation area of the 1998 GLOF. The lake is clearly visible in most images and shows a maximum lake size on the image of 1976. The 1998 images provide the lake outline as of 9 July 1998, i.e. one day after the "Shakhimardan event" occurred. The brown line in the 1976 image indicates the crest of the moraine dam, whereas the blue arrow points to traces of surface runoff. Dates of images and further details are provided in Table 2. (For interpretation of the references to colour in this figure legend, the reader is referred to the web version of this article.)

4.2. Lithodynamic zones: where did all the debris-flow material come from?

In the following we describe the evolution of the GLOF and ensuing flow/flood by describing the disaster along its path downvalley. We do so by presenting the sequence of lithodynamic zones of the 1998 flow path in its upper part, in Fig. 7 and in the following. According to video material and data gathered during the field mission, one can see that the original flood wave generated by the GLOF did only entrain small volumes of debris while flowing over the surface of the moraine complex. In addition, runoff from the lake quickly joined the subsurface channels inside the moraine complex and only appeared again on the surface at the glacier complex terminus. Here, erosional features and deposits point to a rapid transformation of the GLOF into a debris flow in the channel with its unstable and highly erodible bed and banks. The debris flow started with a small initial failure volume which then increased considerably through entrainment of material along its path. The multiple erosion zones illustrated in Fig. 7 explain how a relatively small initial volume (in the order of 100×10^3 m^3) can evolve into a large debris flow with dramatic downstream consequences. According to the field data, in the upper part of the path it was a stony debris-flow with matrix-supported deposits (Fig. 7 photos), but at a distance of 17 km from the source the debris flow has transformed to a debris flood (Fig. 7). Shakhimardan settlement is in an area where the debris flood started to transform into a flash flood.

Zones with significant erosion of loose sediment accounted for only about 19% of the total length of the flow path. Erosion zones are mostly located in the headwaters where bed and bank erosion was favored by steeper slope angles in the main channel (with a mean weighted channel angle in the erosion zones of 6.7°). Noteworthy, however, erosion zones are also found in the lower part of the path and at sites with angles <2°. Here, erosion was limited to narrow channels (like gorges) where peak discharge led to significant bank erosion.

Two-thirds of the flow paths can be described as transit zones (68%); they typically occur in the relatively wide, yet steep parts within the

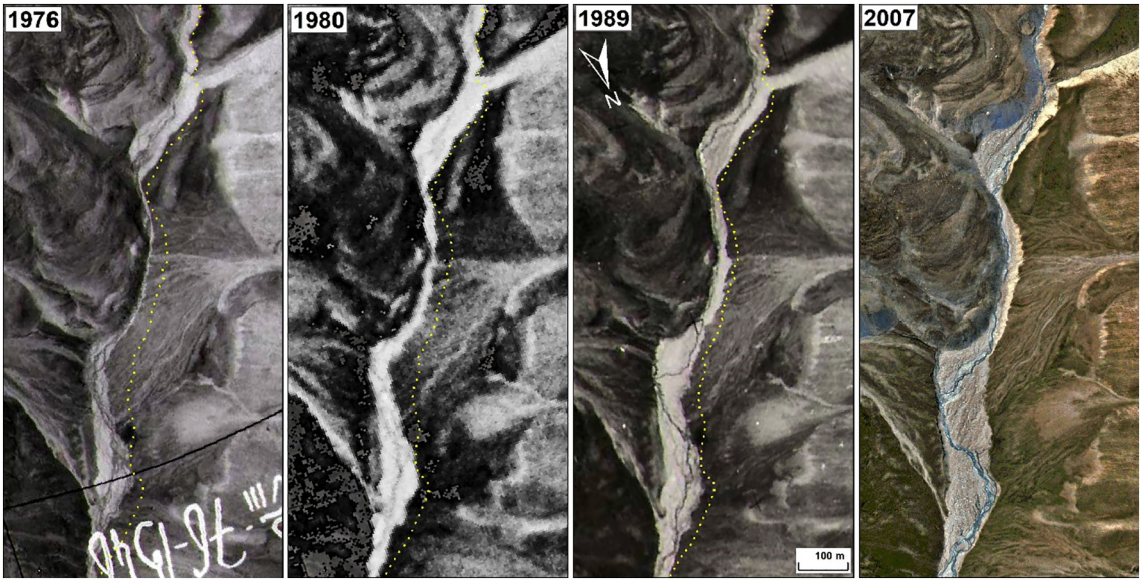

Fig. 5. Changes observed in the main channel of the Allaudin river between 1976 and 2007. The southern (headwater) part of the images is located at a distance of about 2 km downstream of the lake that produced the GLOF in 1998. The margins of the river floodplain as seen in 2007 (right panel) are shown with yellow dots in the other images. The most significant changes occurred between 1989 and 2007, when floodplain area increased by ca. 9500 m^2. Changes observed between 1980 and 1989 were less significant. Exact dates of images and further details on data sources are provided in Table 2. (For interpretation of the references to colour in this figure legend, the reader is referred to the web version of this article.)

river valley. The mean weighted slope angle in the transit and the transit-accumulation zones is 4.2°. Sectors with accumulation can be found only over 2600 m, or < 13% of the flow path. The two major accumulation zones are located at the confluence of the Allaudin with the Karakazyk river and below the confluence of the Archa-Bashi with the Ikedavan river. In addition, two small accumulation zones with channel angles >8° are in the headwaters of the Allaudin river. The mean weighted channel angle of the accumulation zones is 3.5°. Accumulation zones are typically located below steeper parts of the channel, at the valley bottoms of wide sections. The longest accumulation zone is located near the mouth of the Akbek River (Fig. 7).

During the "Shakhimardan event", entrainment of sediments started at the lower end of the moraine complex where the GLOF was forced to pass through a narrow river section due to the presence of two rock glacier lobes; as a result, intense erosion occurred at this segment of the channel. Comparison of images taken in 1989 and 2007 shows that the floodplain area has increased by 9.5×10^3 m^2, with most of these changes induced by the 1998 GLOF. The mean width of the floodplain increased by 17 m, with a maximum increase of ~40 m. With an erosion depth of ~6 m, mean entrainment due to bank erosion can be estimated to 100 m^3/m in this zone. The alternation of erosion/transit/accumulation processes further downstream can be explained by the local channel geometry, whereby bank erosion prevailed in the narrow sections, and bed erosion in the relatively steeper sections with easily erodible material. By contrast, accumulation was typically found in wide, flatter valley sections. Transit zones were generally steeper than accumulation

Fig. 6. Helicopter view of the initiation area of the 1998 disaster. The image was taken on August 1998. Contour of the lake is schematically shown by a red dotted line, whereas the crest of the moraine dam that was eroded during the 1998 event is given with a black line. (For interpretation of the references to colour in this figure legend, the reader is referred to the web version of this article.)

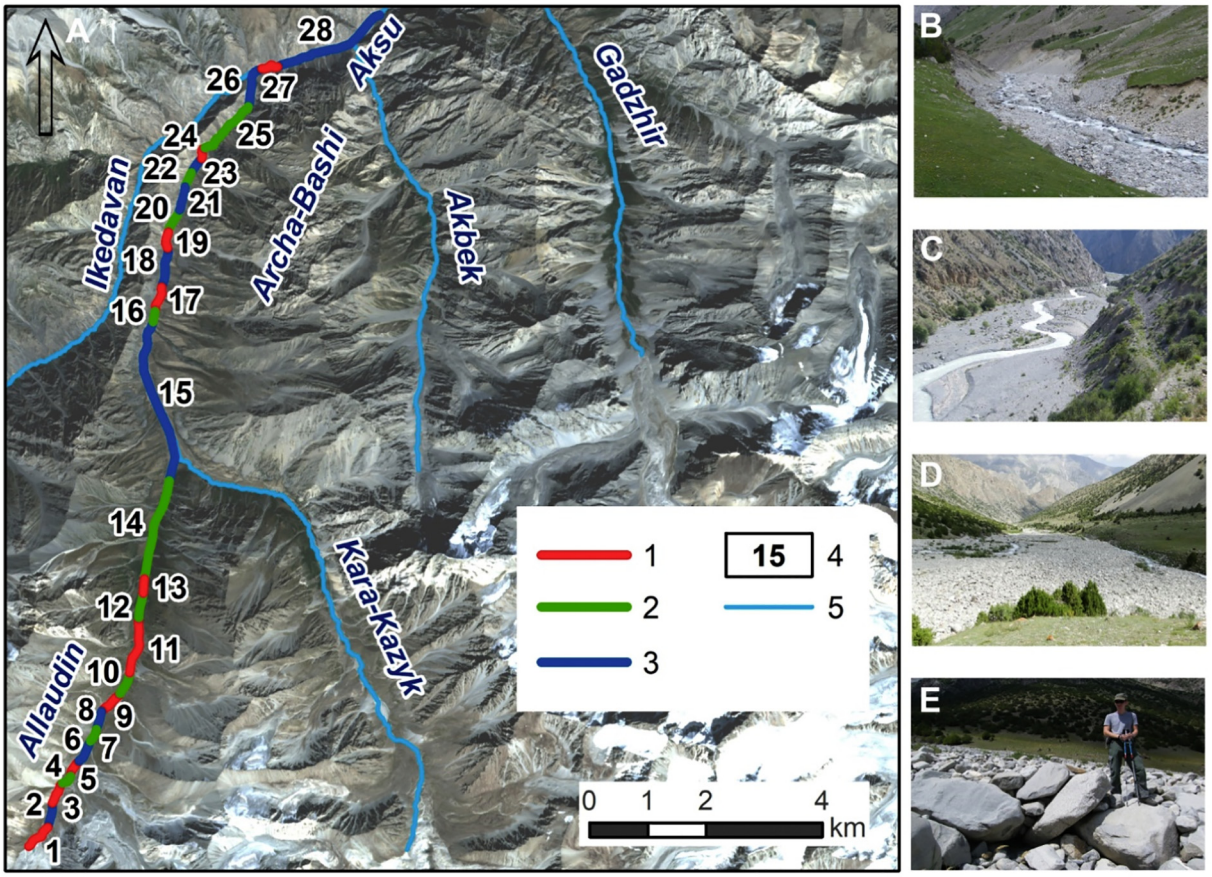

Fig. 7. Lithodynamic zones observed after the passage of the 1998 "Shakhimardan event": overview (A) and illustrative photographs of different zones (B-E) 1 – erosion zone (photo B), 2 – transit-accumulation zone (photo C), 3 – zone of predominant accumulation (photos D, E), 4 – number of the lithodynamic zones identified in the field, 5 – river channels.

zones, yet entrainment remained rather small or even absent in these sectors, likely as a result of the low mobilization potential in these zones.

The main accumulation zones with lengths of 2.8 and 2 km, respectively, are found at the junction of the Karakazyk with the Allaudin river and at the site of an old dammed lake. Depths of debris-flow deposits were assessed as ~2–3 m at the first site but could not be estimated for the second site due to the presence of fluvial sediments covering the 1998 deposits. Downstream from the dammed lake, the debris flow transformed into a flash flood that deposited small accumulation upstream Shakhimardan settlement. These deposits were 20–40 m wide, 50–130 m long and had boulders with sizes of up to 3–5 m.

The volume of transported sediments can be assessed by using the thickness of debris-flow deposits in the accumulation (1.5–2 m) and transit-accumulation zones (0.8–1 m) and was then contrasted against the areas of the accumulation (0.31 km^2) and transit-accumulation (0.25 km^2) zones as mapped on the 2007 Ikonos image. The resulting volume of accumulated debris was thereby estimated as 0.80×10^6 m^3. This value does not include sediments transported out of the study zone by the flash flood. Nonetheless, and despite possible limitations in the approach, it becomes clear that the volume of the Shakhimardan debris flow was significantly smaller than the largest debris flows observed in the Tian Shan (see Table 1) in the 1960s and 1970s.

Flow depths were assessed with evidence left on the debris-flow terraces, resulting in an estimated debris-flow discharge near the confluence of the Karakazyk and Allaudin rivers of about 600 m^3/s, representing a six-fold increase of the initial outburst discharge. Using Kherkheulidze's (1972) equation for debris flows and Golubtsov's (1969) equation for debris floods, mean velocities were 4.5 m/s for the first and 2.2 m/s for the second. The high mobility of the flow also explains why total travel distance of the GLOF and subsequent debris flow and flood exceeded 100 km.

In addition, traces of a temporary lake (with lake deposits on the valley banks) have been found during fieldwork in 2014 (zone 28 in Fig. 7). The role of this lake in the evolution of the 1998 event remains unknown, but it may not have played a major role as water was blocked behind a rock avalanche dam that formed well before 1998 (and as the dam did not fail during the "Shakhimardan event"). Noteworthy, a long zone with significant erosion could be found downstream of the dam, and the presence of the temporary lake may still have played a role in terms of flow dynamics and peak discharge. It is therefore possible that an additional water impulse from the lake may have aggravated severe damage in Shakhimardan.

4.3. Can the Shakimardan disaster repeat in the future? – Inventory of lakes, their outburst potential, and the presence of depressions that may host new lakes in the future

To investigate whether a new disaster could occur in the study region in the future, we assessed the stability of the existing lakes and the potential for new lakes to form in depressions (or sinks) in the periglacial domain, where lakes occur today. The assessment identified 32 lakes in the Shakhimardan catchment (Fig. 8, the full lake inventory is available in Table S1) located at elevations between 1700 and 4300 m a.s.l. If we exclude the two lakes dammed by landslide and alluvial deposits (at 1702 and 1721 m a.s.l.), one notes that lakes are located at altitudes of 4000–4200 m a.s.l., and that only one lake exists above 4200 m a.s.l. (Fig. 9, A).

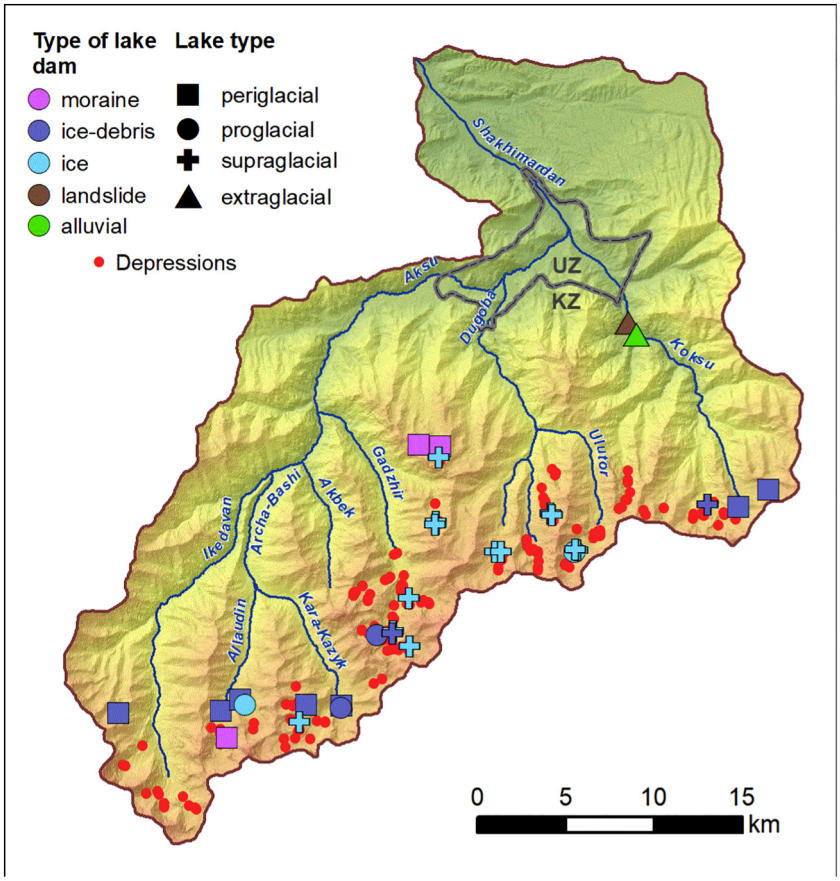

Fig. 8. Mountain lakes and lake-basin depressions of Shakhimardan catchment.

Lake area varies from 400 m^2 to >100,000 m^2, with a mean lake area in the range 5000–10,000 m^2 and a median in in the range 1000–5000 m^2, for a standard deviation of 25,430 m^2. Half of the lakes are supraglacial, roughly one-third are periglacial, 4 (or 13%) are proglacial and 2 (or 6%) extraglacial. In terms of dam type, half of the lakes have ice dams, and one-third of the lakes are dammed by ice and debris (Table 3). The lakes dammed by alluvial and/or landslide deposits are both extraglacial and located at ~1700 m a.s.l. (Fig. 9). For all lakes subsurface drainage appears more important than surface runoff. As a result of significant seismicity in the region and the proximity of lakes to steep bedrock slopes and glacier termini, all but four lakes can possibly be impacted by potential mass movements. The situation is worsened by the fact that the freeboard is <1 m in most cases, except in the case of the 2 extraglacial lakes and one periglacial lake dammed by ancient moraine deposits.

The assessment of outburst potential was limited to the 7 lakes with an area > 5000 m^2 (Table 4), showing that 4 lakes have a high outburst potential. Three of these lakes are supraglacial and the fourth lake is proglacial, but all are dammed by ice and ice-debris dams with a freeboard height < 1 m. Two of them could favor the formation of cascading processes in case of an outburst. One lake has medium outburst potential but could develop into a cascade of processes in case that the periglacial lake dammed by ancient moraine deposits should fail. Yet, under current conditions, the lake has a significant freeboard height, >2 m. The two remaining lakes have a low outburst potential and are located in the extraglacial domain (dammed by landslide and alluvial deposits) with freeboard heights of 14 and 4 m, respectively.

The analysis of depressions yielded information on 171 sinks that are present in the altitudinal range in which dangerous lakes can be found under current conditions. Even if the depressions are not filled with water now, the rapid changes observed in the case of the July 8, 1998 event have shown that the formation and emptying of lakes can occur rapidly and unexpectedly. Therefore, we have to assume that the Shakhimardan catchment has a great potential for the formation of new lakes. At least four of these depressions have an area > 3000 m^2 and could thus become areas of concern should they be filled with water (and affected by thermokarst phenomena) in the future. In conclusion, it seems likely that new lakes with a high outburst potential will appear in the study region in the nearest future.

5. Discussion

In the study reported here, we document remaining evidence of the "Shakhimardan event" which caused a veritable disaster on July 8, 1998 in a village of the same name in Uzbekistan. While political tensions have, for a long time, prevented any detailed post-disaster survey, we have now had the opportunity to visit the site and to reconstruct the origin, dynamics and consequences of the event retrospectively. The distance travelled by the GLOF and subsequent flow and flood processes was close to 100 km and thus significantly higher than the other GLOF events observed in Central Asia (see Table 1 in the Introduction). Its dimensions are, by contrast, comparable to exceptionally large GLOFs documented for the HKH region (Allen et al., 2016; Schwanghart et al., 2016). Without a detailed assessment of the "Shakhimardan event" from 1998, lessons are difficult to be drawn and the disaster could repeat again in the future as several dangerous lakes still exist – or have newly formed – in the catchment, and 171 depressions detected at critical altitudes could fill with water in the future. As such, this contribution provides valuable data on how to better understand the processes that were operating in July 1998, but also to draw some conclusions about the role of the unusual warming episode immediately before the GLOF and subsequent debris flow and debris flood.

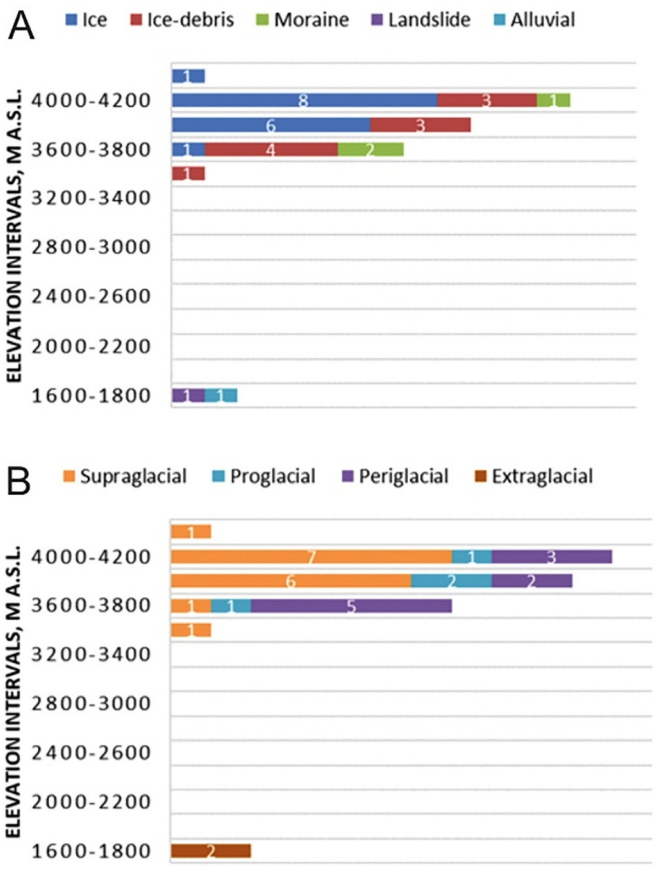

Fig. 9. Distribution of dam types (A) and lake types relative to the glacier (B) by elevation intervals. Note: white numbers indicate the number of lakes in each category.

5.1. Role of weather anomalies

High-magnitude debris flows are often linked with significant weather anomalies, especially intensive rains (e.g., Borga et al., 2014; Schneuwly-Bollschweiler and Stoffel, 2012; Tang et al., 2011; Wieczorek and Glade, 2005), but sometimes are also related to episodes of intense warming and the associated melting of active layer ice in permafrost bodies (Stoffel and Graf, 2015). A literature review shows that temperature extremes clearly are a trigger of GLOFs in periglacial environments (Huggel et al., 2004). As such, GLOFs that were apparently driven by high air temperatures have been reported for recent cases in the Caucasus (Petrakov et al., 2007), Tian Shan (Yafyazova, 2007), Karakoram (Chen et al., 2010) and Tibet (Liu et al., 2014). In the Yarkant catchment (China), Chen et al. (2010) reported a twofold increase of the GLOF frequency and larger peak discharges for the period 1997–2006 as compared to the 1959–1986, and observe these changes primarily after temperature rises. Likewise, Liu et al. (2014) analyzed 24 GLOFs in Tibet and considered that changing air temperatures to be the single most important climate factor for GLOFs; they even reported that all outbursts occurred during the month and days with high average temperatures. Similarly, abrupt rises in air temperatures as well as the occurrence of heatwaves were considered to be among the major GLOF triggering factors in the Gilgit-Baltistan region as well (Din et al., 2014).

In the region investigated here, the Alai Range of Central Asia, direct weather observations are very scarce. At Abramov Glacier, located at a distance of 11 km from the GLOF initiation area, a weather station existed at similar altitude (3837 m a.s.l.), but in a drier context. According to the data available for the 1960s–1970s, mean daily air temperatures at the surface of Abramov Glacier were + 2.6 °C in July, with a probability of occurrence for daily temperatures exceeding +5 °C at 5% (Suslov et al., 1980). According to instrumental data recorded on a moraine next to Abramov glacier, mean daily air temperatures were positive most of June and early July 1998 (Fig. 10). Positive anomalies of +3 °C were measured for July, 3, 1998 and even reached +5.8 °C for July, 7 – July, 8, 1998. Significant positive temperature anomalies for late June and early July are also found in the Berkeley Earth Surface Temperature (BEST) dataset (Rohde et al., 2013), pointing to a positive anomaly of air temperature for 39–40°N and 71–72°E cell in the order of +2.6 °C for July, 3, 1998 and + 3.9 °C for July, 7 – July, 8, 1998. As such, air temperatures near the GLOF site were therefore twice as high as the mean on 7 and 8 July, leading to a much enhanced glacier ablation (Barundun et al., 2015).

In addition, eye witness reports point to a precipitation event immediately before the GLOF and the "presence of black clouds in the mountains". Precipitation was not recorded at the Abramov Glacier weather station, but one has to consider that the station is located in a different orographic context and in a different catchment. The NCEP-NCAR (Kalnay et al., 1996), Era-Interim (Dee et al., 2011) and SMORPH (Joyce et al., 2004) re-analyses datasets do not point to any significant total or daily precipitation during early July, but these products have not been designed to yield information on small-scale, orographic events that are, in addition to their small spatial extent, also very short-lived in many instances. In conclusion, eyewitness evidence exists for the co-occurrence of intense snow and ice melting and a thunderstorm in the catchment, which cannot however be proven by instrumental records or re-analysis products. In any case, the highly positive air temperature anomaly observed prior to the event has favored intensive melting of snow and ice and a subsequent increase of water flowing into the lake (or the depression, which then became a lake). Such weather events are known to lead to a subsequent rise of lake levels and hydrostatic pressures in subsurface channels (Falatkova, 2014). The melting process was, however, short, and discharge data from different rivers in the Alai Range do not point to a significantly higher runoff than average for July 1998. Data on discharge are not unfortunately available for the Shakhimardan River due to the destruction of the gauge by the event.

Table 3
Lake distribution in Shakhimardan River catchment.

	Number of lakes	Percentage of lakes
Dam type		
Ice	16	50
Ice-debris	11	34
Moraine	3	9
Landslide	1	3
Alluvial	1	3
Lake type relative to the glacier		
Supraglacial	16	50
Proglacial	4	13
Periglacial	10	31
Extraglacial	2	6

5.2. Role of parent glacier and rock glacier on GLOF formation

The lake that was at the origin of the GLOF disaster has formed in an intra-moraine depression located in the moraine complex of the Archa-Bashi Glacier. In its upper part, the moraine complex consists of stagnant, debris-rich ice, a remnant of the former snout of Archa-Bashi Glacier. The area of Archa-Bashi Glacier has decreased from 2.5 (Konovalova, 1974) to 1.9 km^2 (our delineation), and its length decreased from 3.4 to 2.3 km due to the stagnation of the lower part of the snout. Noteworthy, delineation of the lower glacier margin is quite uncertain due to absence of any clear boundary between the glacier and the moraine complex. Processes of glacier snout stagnation, expansion of debris cover, formation of thermokarst lakes and depressions are typical for the entire Archa-Bashi Glacier. In 2018 two lakes exist in the

Table 4
Lake parameters and assessment of outburst potential for those lakes with an area > 5000 m^2.

Id	Lake area, m^2	Type of lake	Type of the dam	Free-board, m	Dam geometry[b]	Connec-tion between lakes	Type of drainage	Possible potential for lake impact	Value of outburst potential	Outburst potential
3	5099	S (3)[a]	I/d (2)	<1 (3)	(9)	Single (1)	Under (3)	Ice-fall, avalanche (3)	24	High
4	116,679	E (1)	A (1)	4 (1)	(3)	Cascade (3)	Under (3)	Rock-fall, debris flow (3)	15	Low
5	92,702	E (1)	L (1)	14 (1)	(3)	Cascade (3)	Under (3)	Rock-fall, debris flow (3)	15	Low
12	13,511	S (3)	I (3)	<1 (3)	(9)	Single (1)	Under (3)	Ice-fall (3)	25	High
14	18,525	P (2)	M (2)	2 (1)	(3)	Cascade (3)	Under (3)	Rock-fall, avalanche (3)	17	Medium
22	9774	S (3)	I/d (2)	<1 (3)	(9)	Cascade (3)	Under (3)	Ice-fall, debris flow (3)	26	High
24	10,755	Pr (3)	I/d (2)	<1 (3)	(9)	Cascade (3)	Under (3)	Ice-fall (3)	26	High

[a] Values of the key parameters score are given in brackets: (1), (2) or (3) points.
[b] (9) points in "Dam geometry" column correspond to the lakes with dam freeboard lower than 1 m and (3) points to the lakes with dam freeboard higher than 1 m. We did not measure the geometrical characteristics of these dams due to the low resolution of the remotely sensing data (10 m for the satellite images and 12.5 m for the DEM). Abbreviations: S - supraglacial, E - extraglacial, P - periglacial, Pr - proglacial; I/d - ice-debris, A - alluvial deposits, L - landslide, I - ice, M - moraine; Under - underground.

terminal as well as in the upper parts of the moraine complex; they likely formed during early 2000th. The area of the lakes is currently 4×10^3 m^2 but both lakes are expanding. In addition, in its lower part, the moraine complex coalesces with a rock glacier flowing from the eastern slope into the valley. This rock glacier is not active under current conditions and a thermokarst lake has formed on its surface.

Using the first approach developed by (Huggel et al., 2002), we obtain a lake volume prior to the GLOF on July 8, 1998 of $V = 133 \times 10^3$ m^3, and a post-event volume of ~30×10^3 m^3. Using the second approach developed by (Narama et al., 2018), we define a pre-outburst volume close to 120×10^3 m^3. Whereas both assessments yield quite comparable results we cannot assess their reliability.

Likewise, we attempted to reconstruct the maximum outburst discharge. Assuming an ice dam and using the equation of Haeberli (1983), we obtain $Q_{max} = 133$ m^3/s. By contrast, the equation of Walder and Costa (1996), primarily used for englacial or subglacial drainage, provides $Q_{max} = 12$ m^3/s. This discharge is clearly not enough to provide significant erosion on slopes with angles within 10–14°, so the observations of a breach in the dam and a failure through retroactive erosion during overflow are confirmed by the calculations. Yet, the moraine dam has not been destroyed completely during the GLOF, and clear surficial drainage is still not present from the lake depression, as water nowadays drains through englacial and/or subglacial channels. However, is seems likely that the lake filled quickly during the extremely warm days preceding the event, either as a result of intensive melting alone, the combination of melting and a local thunderstorm, and/or the occurrence of a melt-induced jokulhlaup from the glacier. We therefore suppose that water inflow from the glacierized basin above the lake must have been significant in early July 1998, and that englacial channel(s) were simply not large enough to compensate for the water inflow into the lake depression. At the beginning of the ablation season, subsurface tunnels existing in moraine complexes can be completely or partially blocked by frozen water that accumulatedin these tunnels during winter, or by the collapse of ice and debris around the ice tunnels (Narama et al., 2018). The water level therefore increased to a point where it started to overflow the dam crest. Dam erosion would then have continued until the englacial channel was again able to absorb the incoming flow. It is unlikely that the englacial channel was blocked completely during the GLOF event as the dam would have eroded completely in this case.

5.3. Did mass movements or earthquakes trigger the Shakhimardan GLOF?

Rock avalanches are recognized as an important trigger of GLOF due to the formation of surge waves in lakes and the subsequent overtopping of dams (Hubbard et al., 2005; Ives et al., 2010; Richardson and Reynolds, 2000). At the study site, fresh rock avalanche deposits could be found downstream of the moraine complex where the GLOF occurred on July 8, 1998. The occurrence of the rock avalanche has not been documented and therefore remains unknown. Its deposits (length ~1 km; width ~0.2 km, thickness at least 3 m thick in its terminal part) are visible on the videos shot during helicopter reconnaissance immediately after the event. The presence of snow patches on the deposits, however, does not support an occurrence of the rock avalanche in summer 1998, so the event can, at best, have happened in winter 1997/98, if not before. Therefore, the rock avalanche can be ruled out as a possible trigger of the GLOF

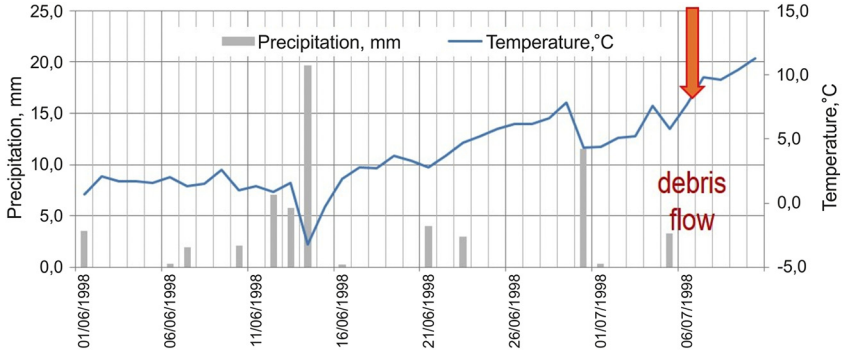

Fig. 10. Air temperatures and precipitation totals recorded at Abramov Glacier weather station located at a distance of 11 km from the GLOF source area between 1 June and 10 July 1998. Data courtesy by Yury Tarasov (NIGMI of UzHydromet, Tashkent), used with permission.

event itself but may have caused a displacement of sediments within the moraine complex and/or a partial destruction of englacial channels. Earthquakes can be ruled out as a possible trigger of the GLOF disaster as well. The low-magnitude earthquake to the south of Kuliab, Tajikistan, on 7 July 1998, at a distance of 270 km from the studied site, was not strong enough to explain the GLOF.

5.4. Entrainment and transport of debris

Debris-flow erosion is generally described to be important for cases in which channel gradients exceed 8° (O'Connor et al., 2001; Huggel et al., 2004). In our case, only 1400 m (or ~36%) of the zones showing strong erosion were steeper than 8°, with a mean weighted channel angle for all zones with significant erosion of 6.7°. Similarly, traces of accumulated debris were absent in the zones characterized by erosion in the Shakhimardan catchment, even in those segments in which channel angles were smaller than the mean. These observations are somewhat in contradiction with current literature where accumulation is described to occasionally occur at slopes of up to 14°, depending on discharge and channel geometry (Huggel et al., 2004; Hungr et al., 1984).

The alternation of erosion and accumulation sections along the river channel is controlled by bed angle, width and availability of easily mobilized sediments. Whereas in the headwaters of the Shakhimardan catchment, significant erosion occurred at bed angles from 7 to 11°, and therefore at bed slopes comparable to those reported in literature (O'Connor et al., 2001), we observed bank erosion in halfway between the GLOF source and Shakhimardan settlement at angles 2.5–4.5°. Also, after transforming into a stony debris flow in the valley headwaters, the mass travelled for another 17.2 km, despite the fact that the flow path had a very low angle of 5.5°.

The high mobility of the flow also explains why the total travel distance of the GLOF and subsequent debris flow and flood exceeded 100 km. This distance is significantly higher than that of all other cases observed in Central Asia, but comparable with exceptional GLOFs in the HKH region (Richardson and Reynolds, 2000; Allen et al., 2016). The travel time of the GLOF from its source to the settlement of Iordan in the Uzbek exclave was thus likely in the order of 3.5 h. Even if this estimate remains very approximate and may possibly underestimate flow velocity, it becomes obvious that an early warning system could have saved numerous lives.

5.5. Uncertainties of lake inventory and outburst potential assessment

On the basis of a Sentinel-2 MSI satellite images taken on 28 August 2018, we identified 32 mountain lakes in our study, with a total surface of 310,966 m^2. The total uncertainty in the lake area assessment was estimated as 47,950 m^2 or 15% and can be ascribed to the resolution of images and consequent errors resulting from image quality and visual interpretation. Comparing current results with previous inventory data based on satellite images obtained in 2009–2014, we detect changes both in the number and total area of lakes: whereas the number of lakes has increased from 24 to 32 lakes (Viskhadzhieva et al., 2016), their mean and median sizes have decreased by 61 and 69% respectively. Noteworthy, changes differ significantly between different types of lakes: whereas total area of near-glacial lakes (i.e. pro-, peri- and extraglacial lakes) did not changed significantly, that of small supraglacial lakes has increased by a factor of 1.5. By contrast, the area of large supraglacial lakes (with areas >5000 m^2) has decreased by a factor of 1.3. Some of these changes are possibly linked to inevitable errors occurring during visual interpretation of remotely-sensed data. On the other hand, however, the growth of small supraglacial lakes can also and reasonably be explained by ongoing climate change and related downwasting of glaciers where unstable glacier lakes have been shown to form (Zaginaev et al., 2016, 2019). Similar observations regarding increasing number and area of lakes have been reported for the Pamir and the Tien Shan mountain regions as well (Mergili et al., 2013; Zheng et al., 2019).

Lake inventories are an important tool for GLOF hazard assessments, but also have their limitations, especially in Central Asia where GLOFs have been initiated repeatedly by rapidly emptying englacial water pockets (Zaginaev et al., 2016) that cannot be identified in remotely-sensed data. In addition, and as illustrated by the differences reported in terms of lake number and area in the catchment within less than ten years, ongoing warming is favoring rapid changes in periglacial environments, and lakes tend to appear and disappear, grow and decrease quite rapidly as well. Consequently, frequent monitoring of environments like the Shakhimardan catchment seems primordial to mitigate existing and evolving GLOF hazards.

6. Conclusions

The Shakhimardan GLOF on July 8, 1998 was the largest known transboundary event in Central Asia. Furthermore, it was the deadliest GLOF in the region in historical times. Investigation of the site that was at the origin of the "Shakhimardan event" showed that the GLOF was initiated as water started to overflow a lake depression that formed on the surface of a moraine complex. This same depression had been occupied temporarily by a lake during the 1970s and 1980s, but no GLOF had been recorded at the site prior to 1998. We conclude that water must have drained through englacial or subglacial channels and that the lake was a typical example of a non-stationary (Erokhin et al., 2018) or short-lived (Daiyrov et al., 2018) lake in Central Asia. In 1998, however, the lake must have filled very quickly, as in the cases of the Zyndan (Narama et al., 2010) or Teztor (Erokhin et al., 2018) lakes, such that the drainage capacity of the englacial channels could no longer evacuate the excessive amounts of meltwater from the Archa-Bashi Glacier, which, in turn, were enhanced by unusually warm air temperatures from relatively cold (June 1998) to extremely warm during the days prior to the event. An abrupt rise in air temperatures has led to formation of GLOFs in Gilgit-Baltistan (Din et al., 2014). This case may serve as a textbook example of GLOF triggering from non-stationary lakes, and helps to explain the situation observed in this study. As a result of the overflowing water, the moraine dam has been partially destroyed by the overflow from the lake until the "water balance" in the depression returned to a level at which the capacity of the englacial channel sufficed again to transfer incoming meltwater from the glacier to the river.

With ongoing climate warming and glacier wasting, further lakes are likely to form in the periglacial environments of Central Asia. 32 lakes were identified in the Shakhimardan River catchment in 2018, four of them have a high outburst potential. The two lakes that emerge in our lake inventory for Archa-Bashi Glacier and moraine complex are just examples of how the high-elevation environments in these regions are evolving and constantly changing. As such, "Shakhimardan" is likely to repeat, be it in the catchment we investigated in this study or elsewhere in the region. We therefore call for the urgent installation of early warning systems at critical sites like the one described here, with data transfers to both the Kyrgyz and Uzbek disaster risk management units, but also to the Sokh and Varukh exclaves for which evidence of debris-flow activity have been registered in the headwaters as well. We conclude that a systematic monitoring of evolving glacier lakes, a constant transfer of data as well as the installation of early warning systems are very crucial to mitigate transboundary impacts of GLOFs, not just in the Ferghana valley, but all across High-Mountain Asia.

Supplementary data to this article can be found online at https://doi.org/10.1016/j.scitotenv.2020.138287.

CRediT authorship contribution statement

Dmitry A. Petrakov: Writing - original draft, Formal analysis, Investigation, Writing - review & editing. **Sergey S. Chernomorets:** Formal analysis, Investigation, Writing - review & editing. **Karina S. Viskhadzhieva:** Formal analysis, Investigation, Writing - review & editing. **Mikhail D. Dokukin:** Formal analysis, Investigation, Writing -

review & editing. **Elena A. Savernyuk:** Formal analysis, Investigation, Writing - review & editing. **Maxim A. Petrov:** Data curation, Writing - review & editing. **Sergey A. Erokhin:** Data curation, Writing - review & editing. **Olga V. Tutubalina:** Writing - original draft, Writing - review & editing. **Gleb E. Glazyrin:** Data curation, Writing - review & editing. **Alyona M. Shpuntova:** Investigation, Writing - review & editing. **Markus Stoffel:** Writing - original draft, Writing - review & editing.

Declaration of competing interest

The authors declare that they have no known competing financial interests or personal relationships that could have appeared to influence the work reported in this paper.

Acknowledgments

This study was funded by the Swiss National Science Foundation (SNF, Schweizerischer Nationalfonds zur Förderung der wissenschaftlichen Forschung) in the framework of the DEFenCC project (n°152301; Future DEbris Flows and lake outburst floods in Tien Shan: possible impacts of projected Climate Change). Data processing was partially funded by the Russian Foundation for Basic Research, project 18-05-00520. We also thank M. Cerny (Geomin, Czech Republic), V. Zaginaev (Kyrgyz State Agency of Geology), E. Ananyeva, G. Uglov (Dugoba montaneering camp, Kyrgyzstan), D. Nikiforov, (Shakhimardan seismological station, Institute of Seismology, Uzbekistan), S. Gavrilova (MSU) for logistical support, valuable information and discussions. We also would like to acknowledge the constructive and helpful comments and suggestions of three anonymous reviewers and Editor-in-Chief Damia Barcelo which greatly improved the quality of the paper.

References

Allen, S.K., Rastner, P., Arora, M., Huggel, C., Stoffel, M., 2016. Lake outburst and debris flow disaster at Kedarnath, June 2013: hydrometeorological triggering and topographic predisposition. Landslides 13 (6), 1479–1491. https://doi.org/10.1007/s10346-015-0584-3.

Allen, S.K., Zhang, G., Wang, W., Yao, T., Bolch, T., 2019. Potentially dangerous glacial lakes across the Tibetan Plateau revealed using a large-scale automated assessment approach. Science Bulletin 64, 435–445. https://doi.org/10.1016/j.scib.2019.03.011.

[dataset] ASF DAAC, 2015. ALOS PALSAR_Radiometric_Terrain_Corrected_low_res; Includes Material © JAXA/METI 2007. Accessed through ASF DAAC. doi:https://doi.org/10.5067/JBYK3J6HFSVF.

Associated Press, 1998. AP archive. http://www.aparchive.com/metadata/Kyrgyzstan-Flooding/c7c3166228226cc339689f849bce797f?query=EXTREME+WEATHER&current=6&orderBy=Relevance&hits=36&referrer=search&search=%2Fsearch%3Fquery%3DEXTREME%2520WEATHER%26allFilters%3DStructural%2520failures%3ASubject&allFilters=Structural+failures%3ASubject&productType=IncludedProducts&page=1&b=ce797f, Accessed date: 22 November 2015.

Bajjali, W., 2017. ArcGIS for Environmental and Water Issues. Springer International Publishing https://doi.org/10.1007/978-3-319-61158-7.

Barundun, M., Huss, M., Sold, L., Farinotti, D., Azisov, E., Salzmann, N., Usubaliev, R., Merkushkin, A., Hoelzle, M., 2015. Reanalysis of seasonal mass balance at Abramov glacier 1968–2014. J. Glaciol. 61 (230), 1103–1117. https://doi.org/10.3189/2015JoG14J239.

Borga, M., Stoffel, M., Marchi, L., Marra, F., Jakob, M., 2014. Hydrogeomorphic response to Extreme rainfall in headwater systems: flash floods and debris flows. J. Hydrol. 518, 194–205. https://doi.org/10.1016/j.jhydrol.2014.05.022.

Brun, F., Berthier, E., Wagnon, P., Kääb, A., Treichler, D., 2017. A spatially resolved estimate of High Mountain Asia glacier mass balances, 2000–2016. Nat. Geosci. 10, 668–673. https://doi.org/10.1038/NGEO2999.

Chen, Y., Xu, C., Chen, Y., Li, W., Liu, J., 2010. Response of glacial-lake outburst floods to climate change in the Yarkant river basin on northern slope of Karakoram Mountains, China. Quat. Int. 226 (1), 75–81. https://doi.org/10.1016/j.quaint.2010.01.003.

Chernomorets, S.S., 2005. Origination Sites of Debris Flow Disaster: Before and after. Nauchniy Mir, Moscow (In Russian).

Daiyrov, M., Narama, C., Yamanokuchi, T., Tadono, T., Kääb, A., Ukita, J., 2018. Regional geomorphological conditions related to recent changes of Glacial Lakes in the Issyk Kul Basin, northern Tien Shan. Geosciences 8 (3), 99. https://doi.org/10.3390/geosciences8030099.

Dee, D.P., Uppala, S., Simmons, A., Berrisford, P., Poli, P., Kobayashi, S., Andrae, U., Balmaseda, M.A., Balsamo, G., Bauer, P., Bechtold, P., Beljaars, A.C.M., van de Berg, L., Bidlot, J., Bormann, N., Delsol, C., Dragani, R., Fuentes, M., Geer, A.J., Haimberger, L., Healy, S.B., Hersbach, H., Hólm, E.V., Isaksen, L., Kållberg, P., Köhler, M., Matricardi, M., McNally, A.P., Monge-Sanz, B.M., Morcrette, J.-J., Park, B.-K., Peubey, C., de Rosnay, P., Tavolato, C., Thépaut, J.-N., Vitart, F., 2011. The ERA-interim reanalysis: configuration and performance of the data assimilation system. Q. J. R. Meteorol. Soc. 137 (656), 553–597. https://doi.org/10.1002/qj.828.

Din, K., Tariq, S., Mahmood, A., Rasul, G., 2014. Temperature and Precipitation: GLOF Triggering Indicators in Gilgit-Baltistan, Pakistan. J. Meteorol. 10 (20), 39–56.

Engel, Z., Sobr, M., Yerokhin, S.A., 2012. Changes of Petrov glacier and its Proglacial Lake in the Akshiirak massif, central Tien Shan, since 1977. J. Glaciol. 58 (208), 388–398. https://doi.org/10.3189/2012JoG11J085.

Erokhin, S., Zaginaev, V., Meleshko, A., Ruiz-Villanueva, V., Petrakov, D., Chernomorets, S., Viskhadzhieva, K., Tutubalina, O., Stoffel, M., 2018. Debris flows triggered from non-stationary glacier Lake outbursts: the case of the Teztor Lake complex (northern Tian Shan, Kyrgyzstan). Landslides 15 (1), 83–98. https://doi.org/10.1007/s10346-017-0862-3.

Falátková, K., 2016. Temporal analysis of GLOFs in high-mountain regions of Asia and assessment of their causes. AUC Geographica 51, 145–154.

Farinotti, D., Longuevergne, L., Moholdt, G., Duethmann, D., Mölg, T., Bolch, T., Vorogushyn, S., Güntner, A., 2015. Substantial glacier mass loss in the Tien Shan over the past 50 years. Nat. Geosci. 8, 716–722. https://doi.org/10.1038/ngeo2513.

Glazyrin, G.E., 1998. Brief Information on the Flood (Debris Flow) Occurred in the Shakhimardan River Catchment on July 8, 1998 (Unpublished Results. (In Russian).

Golubtsov, V.V., 1969. About the hydraulic resistance and formula for calculation of average flow velocity of the mountain Rivers. Proceedings of the Kazakh Scientific Research Hydrometeorological Institute. 33, pp. 30–43 (In Russian).

Haeberli, W., 1983. Frequency and characteristics of glacier floods in the Swiss Alps. Ann. Glaciol. 4, 85–90. https://doi.org/10.3189/S0260305500005280.

Hock, R., Rasul, G., Adler, C., Cáceres, B., Gruber, S., Hirabayashi, Y., Jackson, M., Kääb, A., Kang, S., Kutuzov, S., Milner, Al., Molau, U., Morin, S., Orlove, B., Steltzer, H., 2019. High Mountain areas. In: Pörtner, H.-O., Roberts, D.C., Masson-Delmotte, V., Zhai, P., Tignor, M., Poloczanska, E., Mintenbeck, K., Alegría, A., Nicolai, M., Okem, A., Petzold, J., Rama, B., Weyer, N.M. (Eds.), High Mountain Areas. IPCC Special Report on the Ocean and Cryosphere in a Changing Climate (In Press).

Hoelzle, M., Barandun, M., Bolch, T., Fiddes, J., Gafurov, A., Muccione, V., Saks, T., Shahgedanova, M., 2019. The status and role of the alpine cryosphere in Central Asia. In: Xenarios, S., Schmidt-Vogt, D., Qadir, M., Janusz-Pawletta, B., Abdullaev, I. (Eds.), The Aral Sea Basin: Water for Sustainable Development in Central Asia. Taylor and Francis, London, pp. 100–121.

Hu, Z., Zhang, C., Hu, Q., Tian, H., 2014. Temperature changes in Central Asia from 1979 to 2011 based on multiple datasets. J. Clim. 27 (3), 1143–1167. https://doi.org/10.1175/JCLI-D-13-00064.1.

Hubbard, B., Heald, A., Reynolds, J.M., Quincey, D., Richardson, S.D., Luyo, M.Z., Portilla, N.S., Hambrey, M.J., 2005. Impact of a rock avalanche on a moraine-dammed Proglacial Lake: Laguna Safuna Alta, cordillera Blanca, Peru. Earth Surf. Process. Landf. 30 (10), 1251–1264. https://doi.org/10.1002/esp.1198.

Huggel, C., Kääb, A., Haeberli, W., Teysseire, P., Paul, F., 2002. Remote sensing based assessment of hazards from glacier Lake outbursts: a case study in the Swiss Alps. Can. Geotech. J. 39 (2), 316–330. https://doi.org/10.1139/t01-099.

Huggel, C., Haeberli, W., Kääb, A., Bieri, D., Richardson, S., 2004. An assessment procedure for glacial hazards in the Swiss Alps. Can. Geotech. J. 41 (6), 1068–1083. https://doi.org/10.1139/t04-053.

Hungr, O., Morgan, G.C., Kellerhals, P., 1984. Quantitative analysis of debris hazards for Design of Remedial Measures. Can. Geotech. J. 21 (4), 663–677. https://doi.org/10.1139/t84-073.

ICRC, 1998. Uzbekistan/Kyrgyzstan Floods. https: //reliefweb.int/report/kyrgyzstan/uzbekistankyrgyzstan-floods (accessed 17 October 2019).

IFRC, 2003. Tajikistan appeal no. 01.53/2002 programme update no.02. https://reliefweb.int/report/tajikistan/tajikistan-appeal-no01532002-programme-update-no02, Accessed date: 16 December 2018.

Ives, J.D., Shrestha, B.R., Mool, P.K., 2010. Formation of Glacial Lakes in the Hindu Kush-Himalayas and GLOF Risk Assessment. International Centre for Integrated Mountain Development (ICIMOD), Kathmandu.

Janský, B., Engel, Z., Šobr, M., Beneš, V., Špaček, K., Yerokhin, S., 2009. The evolution of Petrov Lake and Moraine Dam Rupture Risk (Tien-Shan, Kyrgyzstan). Nat. Hazards 50 (1), 83–96. https://doi.org/10.1007/s11069-008-9321-8.

Joyce, R.J., Janowiak, J.E., Arkin, P.A., Xie, P., 2004. CMORPH: a method that produces global precipitation estimates from passive microwave and infrared data at high spatial and temporal resolution. J. Hydrometeorol. 5 (3), 487–503. https://doi.org/10.1175/1525-7541(2004)005<0487:CAMTPG>2.0.CO;2.

Kalnay, E., Kanamitsu, M., Kistler, R., Collins, W., Deaven, D., Gandin, L., Iredel, M., Saha, S., White, G., Woollen, J., Zhu, Y., Chellian, M., Ebisuzaki, W., Higgins, W., Janowiak, J., Mo, K.C., Ropelewski, C., Wang, J., Leetmaa, A., Reynolds, R., Jenne, R., Joseph, D., 1996. The NCEP/NCAR 40-year reanalysis project. Bull. Am. Meteorol. Soc. 77 (3), 437–471.

Kapitsa, V., Shahgedanova, M., Machguth, H., Severskiy, I., Medeu, A., 2017. Assessment of evolution and risks of glacier Lake outbursts in the Djungarskiy Alatau, Central Asia, using Landsat imagery and glacier bed topography Modelling. Nat. Hazards Earth Syst. Sci. 17, 1837–1856. https://doi.org/10.5194/nhess-17-1837-2017.

Kherkheulidze, I.I., 1972. Flow velocities and channel characteristics of the debris flows. Proceedings of Transcaucasian Hydrometeorological Research Institute. 40 (46), 134–180 (In Russian).

Konovalova, G.I. (Ed.), 1974. Glacier Catalog of the USSR. Volume 14. Central Asia. Issue 1. Syr Daria. Part 10. Catchments of the Left Tributaries of the Syr Daria River from Aksu River Mouth and Downstream. Gtdrometeoizdat, Leningrad (In Russian).

Kosarev, M.V., 1954. Glaciers of the Shakhimardan River catchment. Geograficheskiy sbornik 4, 82–89 (In Russian).

Liu, J.J., Cheng, Z.L., Su, P.C., 2014. The relationship between air temperature fluctuation and Glacial Lake Outburst Floods in Tibet, China. Quat. Int. 321, 78–87. https://doi.org/10.1016/j.quaint.2013.11.023.

Medeu, A.R., 2011. Debris Flows in South-Eastern Kazakhstan: Fundamentals of Management. Institute of Geography, Almaty.
Mergili, M., Schneider, J.F., 2011. Regional-scale analysis of Lake outburst hazards in the southwestern Pamir, Tajikistan, based on remote sensing and GIS. Nat. Hazards Earth Syst. Sci. 11, 1447–1462. https://doi.org/10.5194/nhess-11-1447-2011.
Mergili, M., Müller, J.P., Schneider, J.F., 2013. Spatio-temporal development of high-mountain lakes in the headwaters of the Amu Darya River (Central Asia). Glob. Planet. Chang. 107, 13–24. https://doi.org/10.1016/j.gloplacha.2013.04.001.
Mitigating the Adverse Financial Effects of Natural Hazards on the Economies of Central Asia: A Study of Catastrophe Risk Financing Options. World Bank (WB), United Nations Office for Disaster Risk Reduction - Sub-Regional Office for Central Asia (UNDRR SRO CASC), Central Asian Regional Economic Cooperation Program (CAREC).
Narama, C., Duishonakunov, M., Kääb, A., Daiyrov, M., Abdrakhmatov, K., 2010. The 24 July 2008 outburst food at the Western Zyndan Glacier Lake and recent regional changes in Glacier Lakes of the Teskey Ala-Too Range, Tien Shan, Kyrgyzstan. Nat. Hazards Earth Syst. Sci. 10, 647–659. https://doi.org/10.5194/nhess-10-647-2010.
Narama, C., Daiyrov, M., Tadono, T., Yamamoto, M., Kääb, A., Morita, R., Ukita, J., 2017. Seasonal drainage of supraglacial lakes on debris-covered glaciers in the Tien Shan Mountains, Central Asia. Geomorphology 286, 133–142. https://doi.org/10.1016/j.geomorph.2017.03.002.
Narama, C., Daiyrov, M., Duishonakunov, M., Tadono, T., Sato, H., Kääb, A., Ukita, J., Abdrakhmatov, K., 2018. Large drainages from short-lived Glacial Lakes in the Teskey range, Tien Shan Mountains, Central Asia. Nat. Hazards Earth Syst. Sci. 18, 983–995. https://doi.org/10.5194/nhess-18-983-2018.
O'Connor, J.E., Hardison, J.H., Costa, J.E., 2001. Debris Flows from Failures of Neoglacial-Age Moraine Dams in the Three Sisters and Mount Jefferson Wilderness Areas, Oregon. Report No. 1606. US Department of the Interior, US Geological Survey https://doi.org/10.3133/pp1606.
O'Gorman, L., 1996. Subpixel precision of straight-edged shapes for registration and measurement. EEE Transactions on Pattern Analysis and Machine Intelligence 18 (7), 746–751. https://doi.org/10.1109/34.506796.
Petrakov, D.A., Krylenko, I.V., Chernomorets, S.S., Tutubalina, O.V., Krylenko, I.N., Shakhmina, M.S, 2007. Debris flow hazard of glacial lakes in the Central Caucasus. In: Chen, Y., Major, S. (Eds.), Debris-Flow Hazards Mitigation: Mechanics, Prediction, and Assessment. Millpress, Netherlands, pp. 703–714.
Petrakov, D., Shpuntova, A., Aleinikov, A., Kääb, A., Kutuzov, S., Lavrentiev, I., Stoffel, M., Tutubalina, O., Usubaliev, R., 2016. Accelerated glacier shrinkage in the Ak-Shyirak massif, inner Tien Shan, during 2003–2013. Sci. Total Environ. 562, 364–378. https://doi.org/10.1016/j.scitotenv.2016.03.162.
Petrov, M., Sabitov, T., Tomashevskaya, I., Glazirin, G., Chernomorets, S., Savernyuk, E., Tutubalina, O., Petrakov, D., Sokolov, L., Dokukin, M., Mountrakis, G., Ruiz-Villanueva, V., Stoffel, M., 2017. Glacial Lake inventory and Lake outburst potential in Uzbekistan. Sci. Total Environ. 592, 228–242. https://doi.org/10.1016/j.scitotenv.2017.03.068.
Pieczonka, T., Bolch, T., 2015. Region-wide glacier mass budgets and area changes for the central Tien Shan between ~1975 and 1999 using hexagon KH-9 imagery. Glob. Planet. Chang. 128, 1–13. https://doi.org/10.1016/j.gloplacha.2014.11.014.
Radchenko, I., Dernedde, Y., Mannig, B., Frede, H.-G., Breuer, L., 2017. Climate change impacts on runoff in the Ferghana Valley (Central Asia). Water Resources 44 (5), 707–730. https://doi.org/10.1134/S0097807817050098.
Rasul, G., Pasakhala, B., Mishra, A., Pant, S., 2019. Adaptation to mountain cryospheric change: issues and challenges. Climate and Development 16, 1–13. https://doi.org/10.1080/17565529.2019.1617099.
Reuters, 1998. Death Toll in Uzbek Flood Hits 93, Could Go Higher. https://reliefweb.int/report/kyrgyzstan/death-toll-uzbek-flood-hits-93-could-go-higher, Accessed date: 17 October 2019.
Richardson, S.D., Reynolds, J.M., 2000. An overview of glacial hazards in the Himalayas. Quat. Int. 65–66, 31–47. https://doi.org/10.1016/S1040-6182(99)00035-X.
Rohde, R., Muller, R.A., Jacobsen, R., Muller, E., Perlmutter, S., Rosenfeld, A., Wurtele, J., Groom, D., Wickham, C., 2013. A new estimate of the average earth surface land temperature spanning 1753 to 2011. Geoinformatics and Geostatistics: An Overview 1 (1), 1000101. https://doi.org/10.4172/2327-4581.1000101.
Schauwecker, S., Gascón, E., Park, S., Ruiz-Villanueva, V., Schwarb, M., Sempere-Torres, D., Stoffel, M., Vitolo, C., Rohrer, M., 2019. Anticipating cascading effects of Extreme precipitation with pathway schemes – three case studies from Europe. Environ. Int. 127, 291–304. https://doi.org/10.1016/j.envint.2019.02.072.
Schneuwly-Bollschweiler, M., Stoffel, M., 2012. Hydrometeorological triggers of Periglacial debris flows in the Zermatt Valley (Switzerland) since 1864. Journal of Geophysical Research: Earth Surface 117 (F2), F02033. https://doi.org/10.1029/2011JF002262.
Schwanghart, W., Worni, R., Huggel, C., Stoffel, M., Korup, O., 2016. Uncertainty in the Himalayan energy-water Nexus: estimating regional exposure to glacial Lake outburst floods. Environ. Res. Lett. 11 (7), 074005. https://doi.org/10.1088/1748-9326/11/7/074005.
[dataset] Shean, D., 2017. High Mountain Asia 8-Meter DEM Mosaics Derived from Optical Imagery, Version 1. Boulder, Colorado USA. NASA National Snow and Ice Data Center Distributed Active Archive Center. doi:https://doi.org/10.5067/KXOVQ9L172S2.
Sorg, A., Bolch, T., Stoffel, M., Solomina, O., Beniston, M., 2012. Climate change impacts on glaciers and runoff in Central Asia. Nat. Clim. Chang. 2, 725–731. https://doi.org/10.1038/nclimate1592.
Stepanov, B.S., Yafyazova, R.K., 1995. On Climate Influence on the Debris Flow Activity of the Ile Alatau Northern Slope. Hydrometeorology and Ecology. 4 pp. 46–59 (In Russian).
Stepanov, B.S., Yafyazova, R.K., 2001. Radical revision of the debris flow protection strategy is a prerequisite for sustainable development of mountainous and foothill areas of Kazakhstan. Problems of the Hydrometeorology and Ecology, Proceedings of the Scientific-Practical Conference, p. 32 (In Russian).
Stoffel, M., Graf, C., 2015. Debris-flow activity from high-elevation, Periglacial environments. In: Huggel, C., Carey, M., Clague, J., Kääb, A. (Eds.), The High-Mountain Cryosphere: Environmental Changes and Human Risks. Cambridge University Press, Cambridge, pp. 295–314.
Suslov, V.F., Akbarov, A.A., Emelyanov, Yu.N., Nozdrukhin, V.K., Kislov, B.V., Inogamova, S.I., Arapov, P.P., Kharitonov, G.G., Gerasimova, Z.A., Neupokoev, V.A., Aliev, O., 1980. Abramov Glacier (Alai Ridge). Gtdrometeoizdat, Leningrad (In Russian).
Tang, C., Zhu, J., Ding, J., Cui, X.F., Chen, L., Zhang, J.S., 2011. Catastrophic debris flows triggered by a 14 august 2010 rainfall at the epicenter of the Wenchuan earthquake. Landslides 8 (4), 485–497. https://doi.org/10.1007/s10346-011-0269-5.
Tulyaganov, Kh.T., Teush, R.P., Khodzhibaeva, N.N. (Eds.), 1980. Engineering Geology of the USSR. Volume 7. Central Asia. Publishing house of the Moscow State University, Moscow (In Russian).
UNEP, 2007. Global Outlook for Ice and Snow. UNEP/Earthprint.
Vinogradov, Yu.B., 1969. Some questions of the debris flow formation and methods of their estimations. Proceedings of Kazakh Hydrometeorological Research Institute. 33, pp. 5–29 (In Russian).
Viskhadzhieva, K.S., Chernomorets, S.S., Savernyuk, E.A., Tutubalina, O.V., Sokolov, L.S., Erokhin, S.A., Zaginaev, V.V., Petrakov, D.A., Shpuntova, A.M., Dokukin, M.D., Petrov, M.A., Ruiz-Villanueva, V., Stoffel, M., 2016. Debris flows in Alai Mountains and Kyrgyz Range: case studies of Shakhimardan and Aksay Catchments. Debris Flows: Risks, Forecast, Protection, Materials of IV International Conference, pp. 56–59 (In Russian).
Voloshina, A.P., 2002. Meteorology of mountain glaciers. Data of Glaciological Studies 92, 1–240 (In Russian).
Walder, J.S., Costa, J.E., 1996. Outburst floods from glacier-Dammed Lakes: the effect of mode of Lake drainage on flood magnitude. Earth Surf. Process. Landf. 21 (8), 701–723. https://doi.org/10.1002/(SICI)1096-9837(199608)21:8<701::AID-ESP615>3.0.CO;2-2.
Wang, X., Ding, Y., Liu, S., Jiang, L., Wu, K., Jiang, Z., Guo, W., 2013. Changes of Glacial Lakes and implications in Tian Shan, Central Asia, based on remote sensing data from 1990 to 2010. Environ. Res. Lett. 8 (4), 044052. https://doi.org/10.1088/1748-9326/8/4/044052.
Wieczorek, G.F., Glade, T., 2005. Climatic factors influencing occurrence of debris flows. In: Jakob, M., Hungr, O. (Eds.), Debris Flow Hazards and Related Phenomena. Springer, Berlin, Heidelberg, pp. 325–362. https://doi.org/10.1007/3-540-27129-5_14.
World Atlas of Snow and Ice Resources. Russian Academy of Sciences, Moscow (In Russian).
Worni, R., Huggel, C., Stoffel, M., 2013. Glacial Lakes in the Indian Himalayas– from an area-wide glacial lake inventory to on-site and modeling based risk assessment of critical Glacial Lakes. Sci. Total Environ. 468–469, S71–S84. https://doi.org/10.1016/j.scitotenv.2012.11.043.
Yafyazova, R.K., 2007. Nature of Debris Flows in the Zailiysky Alatau Mountains. Problems of Adaptation. Poligrafkombinat, Almaty (In Russian).
Zaginaev, V., Ballesteros-Cánovas, J.A., Erokhin, S., Matov, E., Petrakov, D., Stoffel, M., 2016. Reconstruction of glacial Lake outburst floods in northern Tien-Shan: implications for hazard assessment. Geomorphology 269, 75–84. https://doi.org/10.1016/j.geomorph.2016.06.028.
Zaginaev, V., Petrakov, D., Erokhin, S., Meleshko, A., Stoffel, M., Ballesteros-Cánovas, J.A., 2019. Geomorphic control on regional glacier lake outburst flood and debris flow activity over northern Tien Shan. Glob. Planet. Chang. 176, 5–59. https://doi.org/10.1016/j.gloplacha.2019.03.003.
Zhang, H., Pu, R., Liu, X., 2016. A new image processing procedure integrating PCI-RPC and ArcGIS-spline tools to improve the orthorectification accuracy of high-resolution satellite imagery. Remote Sens. 8 (10), rs8100827. https://doi.org/10.3390/rs8100827.
Zheng, G., Bao, A., Li, J., Zhang, G., Xie, H., Guo, H., Jiang, L., Chen, T., Chang, C., Chen, W., 2019. Sustained growth of high mountain lakes on the headwaters of the Syr Darya River, Central Asia. Glob. Planet. Chang. 176, 84–99. https://doi.org/10.1016/j.gloplacha.2019.03.004.